Influence of nanosilica and a polycarboxylate ether superplasticizer on the performance of lime mortars

J.M. Fernández[a], A. Duran[a], I. Navarro-Blasco[a], J. Lanas[b], R. Sirera[a] , J.I. Álvarez[a*]

[a]*Department of Chemistry and Soil Sciences, School of Sciences, University of Navarra, c/ Irunlarrea, 1, 31008 Pamplona, Spain*

[b]*CTH Navarra, Polígono Talluntxe II C/M, 10, 31192 Tajonar, Spain*

Abstract

The effect of individual and combined addition of both nanosilica (NS) and polycarboxylate-ether plasticizer (PCE) admixtures on aerial lime mortars was studied. The sole incorporation of NS increased the water demand, as proved by the mini-spread flow test. An interaction between NS and hydrated lime particles was observed in fresh mixtures by means of particle size distribution studies, zeta potential measurements and optical microscopy, giving rise to agglomerates. On the other hand, the addition of PCE to a lime mortar increased the flowability and accelerated the setting process. PCE was shown to act in lime media as a deflocculating agent, reducing the particle size of the agglomerates through a steric hindrance mechanism. Mechanical strengths were improved in the presence of either NS or PCE, the optimum being attained in the combined presence of both admixtures that involved relevant microstructural modifications, as proved by pore size distributions and SEM observations.

1. Introduction

The bibliography abounds with examples of the use of admixtures in cement-based materials [1-5]. Various mineral additions have been reported with the aim of improving the technical characteristics of the final product and/or addressing environmental issues [3-5]. The addition of nanosilica (NS) has attracted increasing interest because of the filling effect, which improves the particle size distribution, thus reducing porosity, and the pozzolanic reaction between NS and calcium hydroxide (CH) yielding calcium silicate hydrates (C-S-H). These actions result in enhanced mechanical strength [6-8]. The filling of the interparticle space leads to a denser packing and reduces the water demand, as there is no need to fill the space with water. In this case, the use of a superplasticizer is required in order to guarantee workability [9]. Furthermore, the strong tendency of NS to agglomerate also may make it necessary to use a dispersing additive in order to overcome this problem and to ensure enough reactive surface for the filling effect and C-S-H formation [7,10,11]. Dispersing additives are the so-called plasticizers or superplasticizers, which have a water reducing action on cement materials. When superplasticizers are added, workability at a constant water/cement ratio is improved. Alternatively, the same workability as that of plain cement paste can be reached with an outstanding reduction in water content. In the latter case, cement materials with higher mechanical strengths can be obtained. The adsorption of the plasticizer molecules on the solid particles, either by modifying the surface charge (zeta potential) of the particles, thus increasing the electrostatic repulsion, or by steric hindrance, causes a dispersing action, which has been claimed to be responsible for the increase in fluidity of the cement paste [12]. The interaction between the superplasticizer and the particles of the binder could be affected by the presence of

mineral additions (such as NS, silica fume or fly ash), which means that the compatibility between them needs to be studied [13].

The interest in using lime-based mortars has lately undergone an increase, especially for different applications, such as for rendering mortars or restoring historical monuments [14-19]. Only recently, the performance of aerial lime mortars modified with admixtures has attracted researchers' attention, and the role of water repellents, water retainers, viscosity enhancers and also traditional organic admixtures has been reported in these binding materials [20-27]. The action of superplasticizers on lime mortars has scarcely been considered. Seabra et al. [21] reported the effect on fresh state properties of a sulphonated melamine polymer-based plasticizer, finding a reduction in the water demand and predicting an improvement in mechanical strength. Arizzi and Cultrone [25] have reported improvements on mortar properties upon the addition of a polycarboxylate-based plasticizer blended together with other admixtures in metakaolin-aerial lime mortars. The isolated role of a polycarboxylate ether (PCE) superplasticizer in pure lime mortars, its action mechanism and its effect on mechanical strengths at medium and long-term remain to be established, and they are addressed in this paper. It would also be expected that NS, exhibiting certain pozzolanic behaviour in a similar way to that which takes place when metakaolin is added [19, 25, 28-29], could react in alkaline media with slaked lime particles, giving rise to the formation of calcium silicate hydrates and, therefore, leading to a compressive strength increase. However, the extent of such an interaction, the filling effect of NS as a function of its particle size, and the compatibility between NS and PCE in a lime matrix, need to be clarified. This paper therefore aims to assess the performance of aerial lime mortars modified by the individual or combined addition of two different admixtures: nanosilica and a

superplasticizer based on polycarboxylate ethers. The fresh and hardened state properties in the long term of lime mortars modified by the addition of these admixtures were thoroughly evaluated.

2. Materials and methods

2.1. Materials

Mortars were prepared by mixing a dry slaked lime (class CL 90-S according to Spanish standard [30], supplied by CALINSA, Spain) acting as binder, and a pure limestone aggregate, a calcitic sand, which showed a continuous grading from 0.063 to 1.5 mm. Chemical, mineralogical and grain size distribution of the raw materials were reported elsewhere [20]. The nanosilica was a colloidal silica suspension (pH = 9.68, with a solid/liquid ratio of 0.28) as supplied by ULMEN Europa S.L. (Spain). The superplasticizer was of polycarboxylate ether type, PCE, Melflux 2651F (BASF).

Two different batches of samples were prepared as a function of the binder/aggregate proportion, 1:2 and 1:1 by volume (group of samples denoted as A and B, respectively) (Table 1). These volume ratios were chosen in accordance with previous data that showed the best mechanical strengths and durability performance in aerial and hydraulic lime mortars [14,16,31]. With the aim of avoiding any imprecise measurement, these two volume proportions were converted into weight, resulting in 1:6.7 and 1:3 weight proportions, respectively. Different fresh mortar mixtures were prepared with different amounts of nanosilica and superplasticizer (Table 1). For each type of sample, A or B,

one was composed only of lime and aggregate, and was taken as a reference mortar (samples AC and BC, respectively).

Given that the assayed admixtures were expected to have a strong influence on the consistency of the mortar, each one of the specific dry mixture proportions was prepared in duplicate, altering the water/binder ratio. Samples were denoted with F when the water/lime ratio was fixed to the ratio achieved for good workability in the control samples (1.54 W/B ratio for A mortars and 1.12 W/B for B mortars). In the other case, the samples were nominated with a W, when the water/lime ratio was adjusted to obtain normal consistency and acceptable workability by means of the mini-spread flow test [20,32]. The aim of preparing these two batches of samples as a function of the mixing water was to identify, as far as possible, the effect of each admixture on the water demand (samples F), while, simultaneously also testing workable and, thus, applicable mortars (samples W).

2.2. Methods

2.2.1. Mortars preparation

Lime, aggregate and dry PCE admixture, when necessary, were blended for 5 min using a solid admixtures mixer BL-8-CA (Lleal S.A.). Water (and, if required, nanosilica suspension) was then added and mixed for 90 s at low speed, in a Proeti ETI 26.0072 mixer. For the determination of fresh state properties, mortars settled for 10 min before being tested, to let the additive take effect. Straight afterwards, fresh state measurements were carried out as described below.

For hardened state properties, mortars were moulded in prismatic 40x40x160 mm casts, compacted in a specific automatic compactor for 60 s and stored indoors at 60% RH and 20ºC, and demolded 5 days later [33]. The majority of the samples was tested after 7, 28 and 91 curing days, this last time being a curing period long enough to allow comparisons between aerial lime mortars [14]. Some samples were also tested after 182 and even 365 curing days. Statistical significance of the results obtained was ensured because three specimens were tested at each time for each one of the samples, and the reported results are an average of the obtained results. When deemed necessary, results are presented with error bars corresponding to 1 standard deviation.

2.2.2. Fresh state properties

For the fresh state, several properties were studied. Experimental methods were conducted as follows.

Consistency of the fresh mortar samples was measured through the mini-spread flow test, by measuring the slump after the standardized procedure [32]. Furthermore, viscosity measurements were carried out in lime pastes by means of a HAAKE Viscotester VT 550, with a programme of rotation speeds increasing from 0 to 500 s^{-1} during 90 s. Two batches of samples were tested: the first one was obtained by mixing 20 g of lime and increasing amounts of PCE (from 0 to a maximum of 4 wt.% with respect to lime weight). The second one was prepared by also adding 6 wt.% NS with respect to lime weight. Then, water was added up to 100 mL of suspension.

The water retention capacity was calculated by weighing absorbent materials placed on the fresh sample before and after 5 min of contact under pressure [34].

The open time of the fresh mortars was obtained from a specific device provided with a bradawl, which pushed the fresh sample until the strength exerted to introduce it into the sample was larger than 15 N [35]. In order to confirm the obtained open time results, workable lime pastes (when necessary, modified by the addition of one of the studied admixtures) were also prepared and their setting time measured according to the well-known norm for cements, with Vicat equipment [36].

Specific mixtures of lime, water, and admixture were prepared to assess the zeta potential and the particle size distribution, with a view to elucidating the mechanism through which the admixtures acted.

The determination of zeta potential of solid-liquid interface has been reported to be a valuable method in order to study the action mechanism of admixtures, because the adsorption of some admixtures (such as PCE and other plasticizers) on the solid surface of binder modifies the surface charge of the particles [12,37,38]. With the aim of studying the zeta potential and in accordance with previous studies [24,37,38], solutions of 2 g of dry hydrated lime in 50 mL of water were prepared. Increasing amounts of the PCE were added, thus obtaining different solutions (from 0 to 4 wt.% with respect to lime weight). Six percent of NS was added to one batch of the samples, while the other contained only lime and PCE. Finally, in order to study possible adsorption of PCE onto NS, free-lime suspensions of colloidal NS, in the same amount as the previous batch of samples, with increasing additions of PCE, were studied. After 5 min of stirring, the

mixtures were separated by centrifuge, and the supernatants were analysed using a Zeta Potential Analyzer ZETA PLUS (Brookhaven Instruments Corporation, New York, U.S.A). The average of ten measurements was regarded as the zeta potential of the lime particles.

Furthermore, with a view to studying the behaviour of lime particles in suspensions with the tested admixtures, 20 g of lime was added to 100 mL of water. As in the zeta potential studies, increasing amounts of the PCE were added, thus obtaining different solutions (from 0 to 4 wt.% with respect to lime weight). Six percent of NS was added to one batch of the samples, while the other contained only lime and PCE. The particle size distribution (PSD) of these samples was determined using a Malvern Mastersizer (Malvern Instruments, Ltd., U.K.). Moreover, the PSD of free-lime suspensions of colloidal NS was also studied upon addition of increasing percentages of PCE. The PSD of a plain PCE solution was also measured. Optical microscopy (Olympus CH40, with Color view- soft imaging systems camera) was also used in order to observe the particle size in the above-mentioned suspensions.

2.2.3. Hardened state properties

For the mineralogical characterization of the hardened mortars, samples were ground in an agate mortar to powder and measurements were carried out by powder X-ray diffraction (in a Bruker D8Advance diffractometer - Karlsruhe, Germany-, with a $CuK_{\alpha 1}$ radiation and 0.02º 2θ increment and 1 s·step^{-1}, from 2º to 90º 2θ) and by Fourier Transform Infrared-Attenuated Total Reflectance (FTIR-ATR) spectroscopy, in a Nicolet-Avatar 360 equipment. The resolution was 4 cm^{-1} and the spectra were the result of averaging 100 scans. All measurements were carried out at 20 ± 1 °C. A

Hitachi S-4800 scanning electron microscope (SEM) (Hitachi, Japan), coupled to an EDS detector, was used to study the morphology and microstructure of the samples. Before SEM-EDS analysis, samples were coated with a gold film.

Pore size distribution tests were performed by mercury intrusion porosimetry (MIP), using a Micromeritics AutoPore IV 9500 with a pressure range between 0.0015 and 207 MPa. Pressure, pore diameter and intrusion volume were automatically registered.

The three-point flexural tests were carried out in the mortar specimens using a Frank/Controls 81565 compression machine at low rates of loading (10 $N \cdot s^{-1}$). Flexural strength determination was done on the Ibertest IB 32-112V01. Compression strength tests were executed on the two fragments of each specimen resulted from the flexural tests. This was done on a Proeti ETI 26.0052, and the rate of loading was 50 $N\ s^{-1}$.

3. Results and discussion

3.1. Fresh state properties

3.1.1. Rheological behaviour. Assessment of the interaction between the admixtures and lime particles: effects on the particle size distribution.

Table 2 summarizes the fresh state experimental results. On the consistency (mini spread-flow test), the presence of NS systematically demands a larger amount of mixing water. For a fixed amount of water (samples F), a progressive decrease of flowability is observed as the percentage of NS increases. The slump flow diameter varied from 180

mm in the control AC sample to 165 mm in sample AF11, containing 6 wt.% NS. A much more pronounced effect was observed for B samples, most of which were prepared with a higher ratio of NS (3 and 6 wt.%) added on a larger proportion of lime, thus resulting in a higher NS net amount. As an example, sample BF3, containing 6 wt.% NS, made the slump diameter decrease from 173 mm (BC control sample) to 141 mm.

In cement mortars, a higher water demand has been reported when the specific surface area supplied by the NS rises [7,39]. But, as stated in the introduction, when there is improved packing, the larger amount of free water could lubricate solid particles, thus allowing the fresh paste to flow easily. The latter effect was not observed in the assayed samples: on the contrary, the presence of NS caused a flowability drop. Another mechanism could be put forward which ruins the particle packing. The formation of agglomerates (a reported problem when using nanosized particles) could explain this bad packing [7]. Furthermore, the reported formation of C-S-H-gel increases the water consumption and, as a consequence, the water demand. Particle size distribution measurements and optical microscopy observations, as discussed below, will show the formation of agglomerates upon the addition of NS and simultaneous consumption of the smallest lime particles, thus preventing them, to a certain extent, from filling the intergranular space and increasing the water demand.

Measurements of the PSD were conducted with the aim of clarifying all the above-mentioned facts. In Fig. 1 (a), a plain NS suspension showed a unimodal distribution, with a sharp peak at 0.30 μm particle diameter. Pure lime suspension PSD resulted in a distribution with peaks at 0.30, 10 (the main particle diameter in volume percentage)

and 50 μm. A shoulder at ca. 200 μm was also observed (Fig. 1(b)). However, when NS and lime were mixed, PSD graph depicted a quatrimodal distribution but with inverted intensity of the central peaks. In fact, there was a reduction in the peak at 0.30 μm, a marked drop in the particles with 10 μm of diameter, and a pronounced increase of the third peak, which also underwent a shift towards larger diameters (from 50 to 60 μm). The shoulder at larger particle diameter also appeared at larger diameters (ca. 300 μm) (Fig. 1(b), NS-lime PSD curve). The formation of new larger particles evidenced the interaction between NS and lime particles. Owing to their highly reactive, large surface, NS particles can act as condensation centres, reacting with some lime particles and leading to C-S-H formation [6,11]. This would explain the consumption of the lime particles with 0.30 and 10 μm of diameter and the appearance of larger particles (60 and 300 μm) and, therefore, the increase in water demand upon NS addition.

Optical microscopy observations helped us to confirm these data: Fig. 2 (a) depicts a plain lime suspension, with a network of 10 μm-sized portlandite particles and some agglomerates ranging from 50 to 100 μm of diameter (dark spots on the micrograph). In addition, at higher magnification, a noticeable population of small portlandite particles (0.3 μm) could also be observed (Fig. 2 (b) shows some areas containing several small particles marked with white circles). All these observations are in good agreement with PSD measurements. The incorporation of NS resulted in the formation of denser and larger structure, with the consumption of the smallest particles of lime (Fig. 2(c)).

Flowability of the fresh mortars was clearly improved upon addition of PCE. Sample AF9, with 0.5 wt.% PCE, underwent a 44% of increase in the slump diameter (Table 2). When workability was adjusted, this effect was denoted by a decrease in mixing water

303 requirements (from 1.54 water/binder ration in AC to 1.27 water/binder ratio in
304 AW10)(Table 1). This effect was even noticeable in samples BF5, BF6 and BF8 in spite
305 of the NS being present up to 6 wt.%, in which the presence of PCE rendered slump
306 values beyond the limits of the mini spread-flow test. All these results were confirmed
307 by means of the viscosity measurements carried out in fresh pastes (Fig. 3). The
308 reduction in the slump diameter when NS was added can be related to the viscosity
309 increase (ordinate axis, 0 wt.% PCE). Upon addition of PCE, viscosity decreased and
310 reached a minimum (ranging from 0.5 to 1 wt.% PCE). It seems that a saturation dosage
311 was then achieved in a lime matrix, and higher contents of PCE did not significantly
312 modify the sample's viscosity. Similar response to superplasticizer addition, with the
313 finding of a saturation dosage, was reported in a cement matrix by Fernàndez-Altable
314 and Casanova [40].
315
316 From these data, it turns out to be evident that PCE acted in lime mortars as a water
317 reducing agent that improves the fluidity of the fresh samples, just in the same way as it
318 did in cement-based matrices [41-45], but its action mechanism in lime matrices needs
319 to be elucidated. PCE compounds have been reported to adsorb on the surface of the
320 main mineral phases of a fresh cement paste: C_3S, C-S-H and ettringite. This fact has
321 been reported to be responsible for the observed increase in suspension fluidity, thanks
322 to the steric hindrance caused by PCE molecules [44]. Zeta potential studies have
323 extensively been used for investigating superplasticizer adsorption in cement
324 suspensions. Zeta potential is defined as the electrical potential developed at the solid-
325 liquid interface and represents the potential difference between the surface of the
326 charged particles and the external plane of Helmholtz (according to a widely used
327 electric double layer model) [46]. The higher this potential is with the same polarity, the

stronger the electrostatic repulsion between particles. Conversely, if the zeta potential value of a suspension is close to the iso-electric point (within the range of -15 to +15 mV), particles tend to flocculate [44,46]. Adsorption-desorption phenomena of ions onto/from the particle's surface modify the electrical double layer and can change the zeta potential values and the suspension stability. The interest in knowing the zeta potential behaviour of a lime paste when PCE and NS were incorporated can thus be inferred. These data, together with the particle size distribution of fresh lime pastes, are helpful with a view to explaining the dispersing mechanism observed for PCE, the admixtures' adsorption behaviour and the interactions when the three components were present: NS, PCE and lime.

In Fig. 4, the zeta potential of a pure lime solution was close to +50 mV, in good agreement with previously published data [24]. Calcium ions have been proved to be potential determining ions for charged surfaces [47]. Therefore, in the Ca^{2+} rich lime suspension, the adsorption of calcium ions onto the lime particles justifies the large positive value of zeta potential. Conversely, the pure NS suspension, with a measured pH value of 9.68, showed a zeta potential value close to -50 mV, a similar value to that reported by Sakthivel et al. [46] and Shih et al. [6]. This large negative charge, caused by the deprotonation of silanol groups [48], provoked a marked inter-particle repulsion, preventing NS from agglomeration.

The simultaneous presence of lime particles and NS (a 6 wt.% NS with respect to lime) gave rise to a slight zeta potential drop (down to +30 mV) as a result of the attachment between particles with opposite zeta potential, partially cancelling out the positive value. This lime-NS interaction had necessarily to lead to the formation of larger

353 particles, as proved by means of the particle size distribution (PSD) of the suspensions,
354 previously discussed (Fig. 1(b)).
355
356 The gradual incorporation of PCE caused a decrease in the zeta potential values of both
357 pure lime and NS-lime solutions, proving the interaction between PCE and lime
358 particles. PCE is a negatively charged polyelectrolyte in the alkaline media of both
359 suspensions, so its adsorption onto particles with positive zeta potential led to a zeta
360 potential reduction, and even to a charge inversion. Regarding the C-S-H particles that
361 could be formed in NS-lime solution, their interaction with PCE is also plausible and it
362 has been widely researched by Zingg et al. [44]. In spite of all, it must be noticed that
363 the NS percentage with respect to the lime content was limited, as is the amount of C-S-
364 H formed. However, the interaction between PCE and NS remains uncertain. Despite
365 the fact that the presence of PCE in pure NS suspension altered the zeta potential values
366 (towards less negative values), the PSD of pure NS (Fig. 1(a)), pure PCE (Fig. 1 (c))
367 and mixed NS-PCE suspensions (Fig. 1 (d)) suggested the absence of interaction. In
368 Fig. 1(a), pure NS showed 0.30 μm of particle diameter while 20 μm was the particle
369 diameter for a pure suspension of PCE (Fig. 1(c)). Mixtures of both components showed
370 no different peaks, but presented regular variation of the peaks' intensity: the larger the
371 amount of PCE added, the more pronounced the peak at 20 μm attributed to this
372 component and the lower the intensity of the NS peak (Fig. 1(d)). The observed changes
373 in the zeta potential values of the NS if PCE was added can be due to the lower charge
374 density of PCE molecules with respect to NS: it has been reported that many PCEs
375 exhibit low or even nearly zero anionic charge densities [49]. By direct titration, our
376 PCE showed 1225 ± 23 meq of anionic sites per gram of polymer. According to
377 previously published data of PCE superplasticizers, the assayed PCE could be classed as

relatively low charge anionic density PCE [44,50]. Therefore, the electrophoretic migration of charged particles was different for NS and for PCE, resulting in a different zeta potential value.

When PCE was added, the zeta potential of pure lime and NS-lime suspensions shifted towards values within the limits of -15 to 15 mV (Fig. 4), so particles should tend to flocculate. However, the above-mentioned results of consistency (measured through the flow table test) proved the effectiveness of the plasticizing/dispersing action of the PCE in lime mortars with and without added NS. Furthermore, the PSD of these suspensions also confirmed the dispersing role. In Fig. 1 (e), depicting pure lime suspensions, it can be observed how the larger particles of lime -diameter around 200 μm - disappeared upon the addition of PCE. Moreover, the PSD were shifted towards lower diameter particles as PCE concentration increased, dramatically reducing the population of 50 μm-particles. Although to a lesser extent, NS-lime suspensions (Fig. 1 (f)) behaved similarly, increasing the population of 60 μm-particles at the expense of the large agglomerates of particles of diameter greater than 350 μm. The dispersing role of the PCE was also proved by means of optical microscopy. Fig. 2 (d) clearly shows the disappearance of large agglomerates in comparison with the micrographs of pure lime and NS-lime suspensions (Fig. 2 (a) and (c)).

Therefore, these findings point to the fact that PCE acted as a dispersing agent in lime suspensions (in lime mortars too) mainly through a steric hindrance mechanism rather than an electrostatic repulsion one. Fresh lime mortars are thus sterically stabilized in the presence of PCE, explaining the observed reduction in mixing water requirements and the increased plasticity of the mixture. This mechanism is in line with previous

403 works in cement materials [13,44,49,51], which report steric forces as the essential
404 mechanism for the PCE fluidizing effect.
405
406 **3.1.2. Water retention and setting time**
407
408 On the other hand, the presence of either NS or PCE caused little change, if any, in the
409 water retention capacity of the assayed lime mortars (Table 2). Only slight variations of
410 the retained water could be found in A samples, with 1:2 lime:aggregate ratio. The
411 small variability, in the most cases falling within experimental error, could not be
412 ascribed to any admixture. In B samples, with 1:1 lime:aggregate ratio, the degree of
413 variability turned out to be negligible.
414
415 However, setting time changes arose as a consequence of the addition of the tested
416 admixtures with respect to control mortars (Table 2). A great dispersion of the
417 experimental results must be noted. To a certain extent, this variability can be explained
418 by taking into account the different proportions of added mixing water and the pore
419 structure of the mortar. It must be considered that the setting of lime mortars is a
420 stepwise procedure. There is a first step in which mixing water evaporates, giving rise
421 to a progressive hardening of the material. In the second step, the uptake of CO_2 starts;
422 it dissolves together with portlandite particles, so that carbonation takes place [52,53].
423 As the presence of admixtures modified the mixing water requirements, an increased
424 amount of mixing water (for example, in samples AW6, AW8, BW2 or BW4) as well as
425 a fixed water amount larger than the one necessary for suitable workability (as in
426 samples AF9, BF5, BF6 and BF8) could explain the observed delay in setting time.
427 Similarly, differences between samples A and B arose from the different water demand

(see Table 1, to achieve a normal consistency control AC sample requires a water/binder ratio of 1.54 but 20% of mixing water with respect to dry raw materials, while BC sample shows a water/binder ratio of 1.12 and 28% of mixing water) and from the resulting porosity. As a general trend, the setting time in samples A turned out to be longer than that of samples B.

Low percentages of NS resulted in a setting time increase. High percentages (6%) of NS gave rise to diverse results: a strong reduction in the setting time was observed for samples AF11 and AW12, while a delay in the hardening of the sample must be noticed for BF6 and BF8 samples. The presence of PCE in these last samples, with an excess of mixing water, influences the results obtained. It is evident that setting time depends on several factors, such as the water demand, the binder:aggregate ratio, the pore structure that has an influence on the water evaporation and the possible retention of water and subsequent hardening process as a result of the C-S-H-gel formation. It was not possible to isolate the effect of each individual factor on the results obtained.

Samples BW7 and BW9 showed a slight reduction in the setting time, ranging from 6 to 11% with respect to the BC control sample. A noteworthy reduction of the setting time was seen, with respect to the AC control sample, for AW10, AF11 and AW12 samples by 86%, 44% and 51%, respectively. These samples are characterized by the presence of PCE and a suitable mixing water amount to yield a satisfactory workable mortar (all of them are samples W except sample AF11 that showed adequate workability notwithstanding). This remarkable finding is of great relevance and it is beneficial for the practical application of lime mortars. One of the most well-known drawbacks of lime mortars is their long setting times, which make their usage difficult [14,17,54].

This obstacle is clearly removed by the addition of PCE in mortars with 1:2 binder:aggregate ratio, opening a new research front for the use of plasticizing agents in lime mortar industry. In order to confirm these results, a more accurate measurement of the setting time was carried out in workable lime pastes by means of the Vicat needle assay according to a standardized norm [36]. Workability of the pastes was adjusted within strict limits of the mini-spread flow (175 mm ± 1 mm). For a plain lime paste, the initial setting time was 284 min, and the final setting time was 494 min. The addition of 6 wt.% NS definitely delayed the setting process (initial setting time: 900 min; final setting time: 970 min). However, the addition of PCE shortened the setting time (227 min for initial setting time and 277 min for final setting time, which was thus reduced by as much as 44%), therefore confirming the results discussed above in mortars as well as the usefulness of plasticizing agents for lime mortars.

3.2. Hardened state properties

3.2.1. Influence of the nanosilica addition

Fig. 5 and Fig. 6 show the evaluation of compressive strength in the mortars. The higher the binder:aggregate ratio, the larger the compressive strength. For example, compressive strength after 91 curing days increased from 2.9 Nmm^{-2} in AF11 mortar (1:2) (Fig. 5) to 4.2 Nmm^{-2} in BF3 mortar (1:1) (Fig. 6) both with 6 wt.% NS. Given that, as previously discussed, carbonation has a significant influence on the hardening process, the mechanical strengths increase with the content of lime binder (1:1), in good agreement with previously published data [14,16,25,55].

Additionally, the observed increase in the mechanical strengths of the NS-bearing mortars was also due to the C-S-H formation. As a matter of fact, it was proved that NS particles modified lime mortar, through the reaction between CH particles and reactive SiO_2 forming calcium silicate hydrates (C-S-H) and increasing the average chain length in their internal structure. The broad IR band at around 1100 cm^{-1} is associated with Si-O-Si asymmetric stretching vibrations. A shift of the former band to higher wavenumber (cm^{-1}) was observed in our samples when NS percentage increases (Fig. 7), which means a higher degree of polymerization due to the formation of C-S-H phase [11,56].

A broad reflection found at around 30º (2θ) in the XRD patterns was ascribed to C-S-H phases (Fig. 8). On the other hand, SEM micrographs show different C-S-H structures, made up of honeycomb, fibres and flakes or thin foil shapes (Fig. 9) [25,57].

The increase in NS resulted in greater mechanical strength. For example, in B mortars (1:1), an 83% increase was observed from BF1 sample (with 3 wt.% NS, 2.3 Nmm^{-2}) to BF3 sample (with 6 wt.% NS, 4.2 Nmm^{-2}) both after 91 curing days (Fig. 6). This behaviour can be explained by taking into account two main factors. First, and predominantly, the formation of C-S-H phases, responsible for the observed mechanical strength improvement, in a similar way that occurs in cement mortars [55]. Secondly, in some cases, a noticeable filling effect was detected, so that NS blocked the pores, thus resulting in a reduction in the mean pore size. This fact can be observed in the pore size distribution, Fig. 10 (a), after 91 curing days, for control mortar BC, and BF1 and BF3 samples. The progressive increase in NS (3 wt.% and 6 wt.%, respectively, for BF1 and BF3), shifted the mean pore size towards lower diameters (0.80 μm for BC, 0.55 μm for

503 BF1 and 0.43 μm for BF3). At the same time, the filling effect for the small pores can
504 also be tested when a significant amount of NS is present (BF3 sample). This change in
505 the pore size distribution contributed to the compressive strength rise measured.
506
507 **3.2.2. Influence of the PCE addition**
508
509 Regarding the role of the PCE, its isolated influence on the compressive strength can be
510 seen in results of samples AF9 and AW10 with respect to the control AC sample (Fig.
511 5). The addition of PCE in sample AW10 caused a marked strength increase. This
512 strength rise was especially significant from 182 curing days onwards for compressive
513 strength results (a 58% of increase with respect to control mortar at 182 curing days,
514 and, after one year of curing, compressive strength was twice as much as the control
515 value, increasing from 3.1 Nmm^{-2} up to 6.3 Nmm^{-2}). Flexural strength values showed an
516 early noticeable increase, i.e. after only 28 curing days. The mechanical strength
517 enhancements in AF9 sample were also noticeable but always to a lesser extent than in
518 the AW10 sample. It must be considered that the water demand in AW10 sample was
519 adjusted to obtain a workable mortar, whilst AF9 sample was prepared with an excess
520 of mixing water and its subsequent evaporation gave rise to larger pores than in the
521 AW10 sample. By way of example, Fig. 10 (b) depicts MIP results for these samples
522 after 182 curing days, showing a larger number of pores greater than 1 μm for the AF9
523 sample than for the AW10 sample. This excess of mixing water and the corresponding
524 increase in porosity explain the lower compressive strength values found in the AF9
525 sample with respect to those found in the AW10 sample. After one curing year, the
526 compressive strength in AF9 increased, with respect to control mortar, by almost 50%
527 (from 3.1 up to 4.6 Nmm^{-2}). An increase in flexural strength was also found, always to a

lesser extent than in the AW10 sample, and which was only significant after 91 curing days (Fig. 5).

In any case, the addition of PCE resulted in a mechanical strength improvement of the lime mortars. As discussed above in the fresh state, PCE, acting as a dispersing agent, reduced the water demand, yielding a good workability, and also avoided the formation of agglomerates (Table 2). These facts led to a more compact mortar with a strong reduction of the macropores between 1 and 10 μm, a reduction of mean pore size and of the total porosity – as proved by the reduction in the cumulative intruded mercury and in the area under the MIP curve– by comparison with the control mortar (Fig. 10(b)). SEM observations allowed us to verify a large degree of compactness of the mortar matrix in this case: the microstructure of the lime mortar after carbonation changed greatly in the presence of the PCE (Fig. 11). The carbonated lime showed large aggregates, which are based on rounded tightly agglomerated crystals of submicrometer-size [58]. The presence of PCE had a major influence on the crystal nucleation and growth process, which promoted the aggregation of calcite crystals. The textural characteristics showed reduced porosity, and, on the other hand, the growing of calcite crystals resulted in a more homogeneous and continuous matrix, allowing the aggregate particles to be embedded. All these microstructural modifications explain the mechanical strength increase.

3.2.3. Influence of the combined action of NS and PCE

The observed improvements in mechanical strengths were even more outstanding upon simultaneous addition of both PCE and NS, as can be observed in Fig. 6 for BF6, BW7,

BF8 and BW9, all of them including 6% wt. NS and variable amounts of PCE. Mechanical strength increases in both compressive and flexural tests were measured with respect to BC control mortar, being significant from 28 curing days onwards. For the BW9 sample, even after 7 days of curing the flexural and compressive strength improvements were significant, reaching values as high as 12.7 Nmm^{-2}, which is more than four-fold the compressive strength value of the control BC sample (3 Nmm^{-2}) after 182 curing days. The need for and the advantage of the addition of a suitable amount of NS in this combined action of both admixtures in order to improve the mechanical performance of the aerial lime mortar can be easily inferred from the different strength values of BF5 (with only 2 wt.% NS) and BF6 (with 6 wt.% NS), both having 0.5% of PCE in their composition. For the former sample, compressive and flexural strengths were even lower than those of the control mortar, while a significant strength increase was found for the BF6 sample.

When appropriate dosages of the admixtures were added, the combined action of both PCE and NS admixtures had a synergistic effect, thus enhancing the strength. Fig. 10 (c) depicts MIP results for these samples after 91 and 182 curing days. The results were very similar and reproducible irrespective of the curing period. A clear, systematic reduction of the mean pore size can be seen: 0.80 μm for the control mortar, BC sample; 0.55 μm for BF8 sample with an excess of mixing water; 0.43 μm for BW7 sample and, finally, 0.22 μm for BW9 sample. This strong reduction in the mean pore diameter was accompanied by a parallel reduction in porosity, demonstrated by a reduction in the area under the curve. Both facts suggest a densification of the matrix, which can be correlated with the observed mechanical strength improvements. These changes in the pore size distribution and porosity were the combined result of the aforementioned

reduction in pore size owing to the presence of PCE, together with the filling effect of NS and the C-S-H formation. SEM micrographs confirmed the observation of a denser matrix for the BW9 sample (Fig. 12 (a) and (d)). In this case, C-S-H structures prevailed over the calcite crystallization obtained in the presence of PCE. Fig. 12 (b) depicts honeycomb-shaped C-S-H, together with some spare rods. In Fig. 12 (c) some areas of C-S-H included within its structure some agglomerates of rounded calcite crystals like those described for PCE-lime mortars. This microstructure of reduced porosity was responsible for the huge increase in compressive strength (107% for the BW7 sample (0.5 wt.% PCE) with respect to the BC sample after one curing year and 323% for the BW9 sample (1 wt.% PCE)) as shown in Fig. 6.

4. Conclusions

The role of nanosilica and a superplasticizer based on polycarboxylate ether when incorporated as admixtures to aerial lime-based mortars has been ascertained. The presence of NS was found to increase the water demand of a lime mortar. In the fresh mixture, NS reacted with small portlandite particles, giving rise to the formation of large agglomerates, as proved by optical microscopy, PSD and zeta potential measurements.

Conversely, the flowability of lime mortars was enhanced by the PCE addition according to the mini-spread flow test. However, viscosity measurements showed a saturation dose of PCE (at ca. 1 wt.% with respect to lime weight) beyond which there is no increase in fluidity. An interaction between hydrated lime particles (positively charged) and PCE (a negatively charged polyelectrolyte) was proved: the gradual

603 incorporation of PCE into lime suspensions caused a decrease in the zeta potential value
604 down to values close to zero. Despite the fact that the zeta potential values suggested
605 that lime-PCE suspension should tend to flocculate, PSD and optical microscopy
606 confirmed the dispersing action and deflocculation caused by the PCE. A steric
607 hindrance was proposed as the main action mechanism of PCE in lime media. In
608 mortars in which both NS and PCE were simultaneously present, the plasticizing action
609 of PCE could also be observed. The experimental results indicated the absence of any
610 interaction between PCE and NS particles.
611
612 Setting time measurements in lime mortars showed that the presence of NS caused
613 variability in the hardening process: in some cases, unlike cement mortars, NS delayed
614 it. However, the PCE addition resulted, as a general trend, in a strong setting time
615 reduction. This finding is of great relevance in order to overcome one of the main
616 disadvantages of the use of aerial lime mortars, which is related to their long setting.
617
618 Mechanical strengths of the aerial lime mortars were improved by the addition of
619 significant amounts of NS ($\geq$ 3 wt.%). This was due to the formation of C-S-H and a
620 filling effect of the NS, enhancing the densification of the binding matrix, as shown by
621 MIP tests. C-S-H gel was detected by FTIR and different C-S-H structures (honeycomb,
622 rods pattern and flakes) were observed by means of SEM.
623
624 The isolated action of PCE produced a noticeable increase in the mechanical strength of
625 the mortars as a consequence of a reduction in the water demand, which resulted in a
626 smaller mean pore size and a larger degree of compactness of the binding matrix. PCE

presence also dramatically changed the microstructure of the carbonated mortar, which showed large agglomerates of rounded, submicrometer-sized calcite crystals.

The highest mechanical performance of the tested lime mortars was obtained under the combined action of both NS, added in appropriate amount, and PCE admixtures. The mechanical improvement was related to a pronounced reduction in the mean pore size and in the porosity. After a 182-day period of curing, a sample containing both admixtures quadrupled the compressive strength value of the control mortar, reaching 12.7 Nmm^{-2}, which is among the greatest values so far reported for aerial lime mortars [14,25,31,59], taking into account that only 6 wt.% NS was added, the only admixture with certain pozzolanic activity.

This work opens up the possibility of exploring improvements in the use of aerial lime mortars, by varying the ratio of admixtures, by adding other pozzolanic admixtures or NS in larger amounts and, possibly, by incorporating superplasticizers of different composition and nature.

Acknowledgements

The authors want to thank CTH Navarra and Calinsa S.A. Navarra for the material supplied. They also gratefully acknowledge Dr. M.C. Jiménez de Haro (ICMS) for her assistance in the SEM analysis. This work was funded by Fundación Universitaria de Navarra under grant FUNA2010-15108152.

References

[1] M. Lachemi, K.M.A. Hossain, V. Lambros, P.C. Nkinamubanzi, N. Bouzoubaâ, Performance of new viscosity modifying admixtures in enhancing the rheological

properties of cement paste, Cem. Concr. Res. 34 (2004) 185-193.

[2] A. Yahia, K.H. Khayat Experiment design to evaluate interaction of high-range water-reducer and antiwashout admixture in high-performance cement grout, Cem. Concr. Res. 31 (2001) 749-757.

[3] C.F. Ferraris, K.H. Obla, R. Hill The influence of mineral admixtures on the rheology of cement paste and concrete, Cem. Concr. Res. 31 (2001) 245-255

[4] X. Shi, Z. Yang, Y. Liu, D. Cross Strength and corrosion properties of Portland cement mortar and concrete with mineral admixtures, Constr. Build. Mater. 25 (2011) 3245-3256.

[5] J.L Gallias, R Kara-Ali, J.P Bigas, The effect of fine mineral admixtures on water requirement of cement pastes, Cem. Concr. Res. 30 (2000) 1543-1549.

[6] J-Y. Shih, T-P. Chang, T-C. Hsiao, Effect of nanosilica on characterization of Portland cement composite, Mat. Sci. Eng. A-Struct. 424 (2006) 266–274.

[7] G. Quercia, G. Hüsken, H.J.H. Brouwers Water demand of amorphous nano silica and its impact on the workability of cement paste, Cem. Concr. Res. 42 (2012) 344-357.

[8] M-H. Zhang, J. Islam, Use of nano-silica to reduce setting time and increase early strength of concretes with high volumes of fly ash or slag, Constr. Build. Mater. 29 (2012) 573-580.

[9] J. Plank, C. Schroefl, M. Gruber, M. Lesti, R. Sieber, Effectiveness of Polycarboxylate Superplasticizers in Ultra-High Strength Concrete: The Importance of PCE Compatibility with Silica Fume, J. Adv. Concr. Technol. 7 (2009) 5-12.

[10] L. Senffa, D. Hotza, W.L. Repette, V.M. Ferreira, J.A. Labrincha, Mortars with nano-SiO2 and micro-SiO2 investigated by experimental design, Constr. Build. Mater. 24 (2010) 1432–1437.

[11] J. Björnström, A. Martinelli, A. Matic, L. Börjesson, I. Panas, Accelerating effects of colloidal nano-silica for beneficial calcium–silicate–hydrate formation in cement, Chem. Phys. Lett. 392 (2004) 242-248.

[12] A. Papo, L. Piani, Effect of various superplasticizers on the rheological properties of Portland cement pastes, Cem. Concr. Res. 34 (2004) 2097–2101.

[13] O. Burgos-Montes, M. Palacios, P. Rivilla, F. Puertas Compatibility between superplasticizer admixtures and cements with mineral additions, Constr. Build. Mater. 31 (2012) 300-309.

[14] J. Lanas, J.I. Alvarez-Galindo, Masonry repair lime-based mortars: factors affecting the mechanical behaviour, Cem. Concr. Res. 33 (2003) 1867-1876.

[15] G. Margalha, R. Veiga, A. Santos Silva, J. de Brito, Traditional methods of mortar preparation: The hot lime mix method, Cem. Concr. Compos. 33 (2011) 796-804.

[16] J. Lanas, R. Sirera, J.I. Alvarez, Study of the mechanical behaviour of masonry repair lime-based mortars cured and exposed under different conditions, Cem. Concr. Res. 36 (2006) 961-970.

[17] C. Rodriguez-Navarro, E. Hansen, W.S. Ginell, Calcium hydroxide crystal evolution upon aging of lime putty, J. Am. Ceram. Soc. 81 (1998) 3032–3034.

[18] P. Faria, F. Henriques, V. Rato, Comparative evaluation of lime mortars for architectural conservation, J. Cult. Herit. 9 (2008) 338-346.

[19] A. Sepulcre-Aguilar, F. Hernández-Olivares, Assessment of phase formation in lime-based mortars with added metakaolin, Portland cement and sepiolite, for grouting of historic masonry, Cem. Concr. Res. 40 (2010) 66-76.

[20] A. Izaguirre, J. Lanas, J.I. Alvarez, Effect of water-repellent admixtures on the behaviour of aerial lime-based mortars, Cem. Concr. Res. 39 (2009) 1095-1104.

[21] M.P. Seabra, H. Paiva, J.A. Labrincha, V.M. Ferreira, Admixtures effect on fresh state properties of aerial lime based mortars, Constr. Build. Mater. 23 (2009) 1147-1153.

[22] A. Izaguirre, J. Lanas, J.I. Alvarez, Ageing of lime mortars with admixtures: Durability and strength assessment, Cem. Concr. Res. 40 (2010) 1081-1095.

[23] A. Izaguirre, J. Lanas, J.I. Alvarez, Characterization of aerial lime-based mortars modified by the addition of two different water-retaining agents, Cem. Concr. Compos. 33 (2011) 309-318.

[24] A. Izaguirre, J. Lanas, J.I. Alvarez, Behaviour of a starch as a viscosity modifier for aerial lime-based mortars, Carbohyd. Polym. 80 (2010) 222-228.

[25] A. Arizzi, G. Cultrone, Aerial lime-based mortars blended with a pozzolanic additive and different admixtures: A mineralogical, textural and physical-mechanical study, Constr. Build. Mater. 31 (2012) 135-143.

[26] L. Ventolà, M. Vendrell, P. Giraldez, L. Merino, Traditional organic additives improve lime mortars: New old materials for restoration and building natural stone fabrics, Constr. Build. Mater. 25 (2011) 3313-3318.

[27] G. Wei, H. Zhang, H. Wang, S. Fang, B. Zhang, F. Yang, An experimental study on application of sticky rice–lime mortar in conservation of the stone tower in the Xiangji Temple, Constr. Build. Mater. 28 (2012) 624-632.

[28] C. Fortes-Revilla, S. Martínez-Ramírez, M.T. Blanco-Varela, Modelling of slaked lime–metakaolin mortar engineering characteristics in terms of process variables, Cem. Concr. Compos. 28 (2006) 458-467.

[29] E. Aggelakopoulou, A. Bakolas, A. Moropoulou, Properties of lime–metakolin mortars for the restoration of historic masonries, Appl. Clay Sci. 53 (2011) 15-19.

[30] EN 459-1, Building lime. Part 1: definition, specification and conformity criteria (2001).

[31] J. Lanas, J.L. Perez Bernal, M.A. Bello, J.I. Alvarez, Mechanical properties of masonry repair dolomitic lime-based mortars, Cem. Concr. Res. 36 (2006) 951–960.

[32] EN 1015–3, Methods of test for mortar for masonry. Part 3: Determination of consistence of fresh mortar (by flow table) (2000).

[33] EN 1015–11, Methods of test for mortar for masonry. Part 11: Determination of flexural and compressive strength of hardened mortar (2000).

[34] UNE 83816:93, Test methods. Mortars. Fresh mortars. Determination of water retentivity (1993).

[35] EN 1015–9, Methods of test for mortar for masonry. Part 9: Determination of workable life and correction time of fresh mortar (2000).

[36] EN 196-3: 2005 + A1: 2009, Methods of testing cement. Determination of setting time and soundness (2005).

[37] D.F. Zhang, B.Z. Ju, S.F. Zhang, J.Z. Yang, The study on the synthesis and action mechanism of starch succinate half ester as water-reducing agent with super retarding performance, Carbohyd. Polym. 71 (2008) 80–84.

[38] D.F. Zhang, B.Z. Ju, S.F. Zhang, L. He, J.Z. Yang, The study on the dispersing mechanism of starch sulfonate as a water-reducing agent for cement, Carbohyd. Polym. 70 (2007) 363–368.

[39] L. Senff, J.A. Labrincha, V.M. Ferreira, D. Hotza, W.L. Repette, Effect of nano-silica on rheology and fresh properties of cement pastes and mortars, Constr. Build. Mater. 23 (2009) 2487-2491.

[40] V. Fernàndez-Altable, I. Casanova, Influence of mixing sequence and superplasticiser dosage on the rheological response of cement pastes at different temperatures, Cem. Concr. Res. 36 (2006) 1222-1230.

[41] S. Chandra, J. Björnström, Influence of superplasticizer type and dosage on the slump loss of Portland cement mortars—Part II, Cem. Concr. Res. 32 (2002) 1613-1619.

[42] A. Zingg, F. Winnefeld, L. Holzer, J. Pakusch, S. Becker, R. Figi, L. Gauckler, Interaction of polycarboxylate-based superplasticizers with cements containing different C3A amounts, Cem. Concr. Compos. 31 (2009) 153-162.

[43] N. Mikanovic, C. Jolicoeur, Influence of superplasticizers on the rheology and stability of limestone and cement pastes, Cem. Concr. Res. 38 (2008) 907-919.

[44] A. Zingg, F. Winnefeld, L. Holzer, J. Pakusch, S. Becker, L. Gauckler, Adsorption of polyelectrolytes and its influence on the rheology, zeta potential, and microstructure of various cement and hydrate phases, J. Colloid. Interf. Sci. 323 (2008) 301-312.

[45] L. Ferrari, J. Kaufmann, F. Winnefeld, J. Plank, Interaction of cement model systems with superplasticizers investigated by atomic force microscopy, zeta potential, and adsorption measurements, J. Colloid. Interf. Sci. 347 (2010) 15-24.

[46] S. Sakthivel, Venkatesan V. Krishnan, B. Pitchumani, Influence of suspension stability on wet grinding for production of mineral nanoparticles, Particuology 6 (2008) 120-124.

[47] H. Viallis-Terrisse, A. Nonat, J.-C. Petit, Zeta-Potential Study of Calcium Silicate Hydrates Interacting with Alkaline Cations, J. Colloid. Interf. Sci. 244 (2001) 58-65.

[48] I. Pointeau, P. Reiller, N. Macé, C. Landesman, N. Coreau, Measurement and modeling of the surface potential evolution of hydrated cement pastes as a function of degradation, J. Colloid. Interf. Sci. 300 (2006) 33-44.

[49] J. Plank, B. Sachsenhauser, J. de Reese, Experimental determination of the thermodynamic parameters affecting the adsorption behaviour and dispersion effectiveness of PCE superplasticizers, Cem. Concr. Res. 40 (2010) 699-709.

[50] J. Plank, B. Sachsenhauser, Experimental determination of the effective anionic charge density of polycarboxylate superplasticizers in cement pore solution, Cem. Concr. Res. 39 (2009) 1-5.

[51] J. Plank, C. Hirsch, Impact of zeta potential of early cement hydration phases on superplasticizer adsorption, Cem. Concr. Res. 37 (2007) 537-542.

[52] M. Arandigoyen, B. Bicer-Simsir, J.I. Alvarez, D.A. Lange, Variation of microstructure with carbonation in lime and blended pastes, Appl. Surf. Sci. 252 (2006) 7562-7571.

[53] M. Arandigoyen, J.I. Alvarez, Carbonation process in lime pastes with different water/binder ratio, Mater. Constr. 56 (2006) 5-18.

[54] M. Arandigoyen, J.I. Alvarez, Blended pastes of cement and lime: Pore structure and capillary porosity, Appl. Surf. Sci. 252 (2006) 8077-8085.

[55] M. Arandigoyen, J.I. Alvarez, Pore structure and mechanical properties of cement–lime mortars, Cem. Concr. Res. 37 (2007) 767-775.

[56] M.Y.A. Mollah, W. Yu, R. Schennach, D.L. Cocke, A Fourier transform infrared spectroscopic investigation of the early hydration of Portland cement and the influence of sodium lignosulfonate, Cem. Concr. Res. 30 (2000) 267-273.

849 [57] R.B. Lin, S.M. Shih, C.F. Liu, Characteristics and reactivities of Ca(OH)2/silica
850 fume sorbents for low-temperature flue gas desulfurization, Chem. Eng. Sci. 58 (2003)
851 3659-3668.
852
853 [58] L. Mo, D.K. Panesar, Effects of accelerated carbonation on the microstructure of
854 Portland cement pastes containing reactive MgO, Cem. Concr. Res. (2012),
855 doi:10.1016/j.cemconres.2012.02.017.
856
857 [59] I. Papayianni, M. Stefanidou. Strength–porosity relationships in lime–pozzolan
858 mortars, Constr. Build. Mater. 20 (2006) 700-705.

Table 1. Mix proportions of the studied samples of lime mortars

SAMPLE	*Lime:Sand ratio (by volume)*	*Lime:Sand ratio (by weight)*	*NS[a] (wt. %)*	*PCE[a] (wt. %)*	*Fixed water (W/B[b] ratio)*	*Adjusted workability (W/B[b] ratio)*
AC (control)	1:2	1:6.7	-	-		1.54
AF1	1:2	1:6.7	0.5	-	1.54	
AW2	1:2	1:6.7	0.5	-		1.54
AF3	1:2	1:6.7	1	-	1.54	
AW4	1:2	1:6.7	1	-		1.54
AF5	1:2	1:6.7	2	-	1.54	
AW6	1:2	1:6.7	2	-		1.69
AF7	1:2	1:6.7	3	-	1.54	
AW8	1:2	1:6.7	3	-		1.69
AF9	1:2	1:6.7	-	0.5	1.54	
AW10	1:2	1:6.7	-	0.5		1.27
AF11	1:2	1:6.7	6	-	1.54	
AW12	1:2	1:6.7	6	-		1.69
BC (control)	1:1	1:3	-	-		1.12
BF1	1:1	1:3	3	-	1.12	
BW2	1:1	1:3	3	-		1.20
BF3	1:1	1:3	6	-	1.12	
BW4	1:1	1:3	6	-		1.32
BF5	1:1	1:3	2	0.5	1.12	
BF6	1:1	1:3	6	0.5	1.12	
BW7	1:1	1:3	6	0.5		0.94
BF8	1:1	1:3	6	1	1.12	
BW9	1:1	1:3	6	1		0.80

[a] Values are expressed in wt. % of NS or PCE with respect to the weight of lime
[b] W/B: Water/binder ratio, i.e. water/aerial lime ratio

Table 2. Consistency, water retention and open time of the studied mortars.

SAMPLE	*Slump (mm)*[a]	*Water retention (%)*	*Open time (hours)*
AC (control)	180	97.8	30.2
AF1	179	96.9	56.9
AW2	179	96.9	56.9
AF3	177	96.4	141
AW4	177	96.4	141
AF5	168	94.6	105
AW6	179	94.2	56
AF7	164	94.9	72.7
AW8	172	95.9	72.6
AF9	260	92.7	49.5
AW10	171	98.3	4.1
AF11	165	94.5	16.8
AW12	176	92.7	14.7
BC (control)	173	97.5	4.1
BF1	165	98.7	6.7
BW2	176	97.8	57.1
BF3	141	97.4	8.4
BW4	178	96.0	18.6
BF5	Excess[b]	98.6	145.7
BF6	Excess[b]	95.0	23.4
BW7	177	97.5	3.7
BF8	Excess[b]	95.6	27.4
BW9	177	98.9	3.8

[a] Consistency was assessed by means of the mini-spread flow test, which measured the slump in the flow table
[b] The flowability of these samples was so large that they flowed beyond the limits of the table

Figure 1

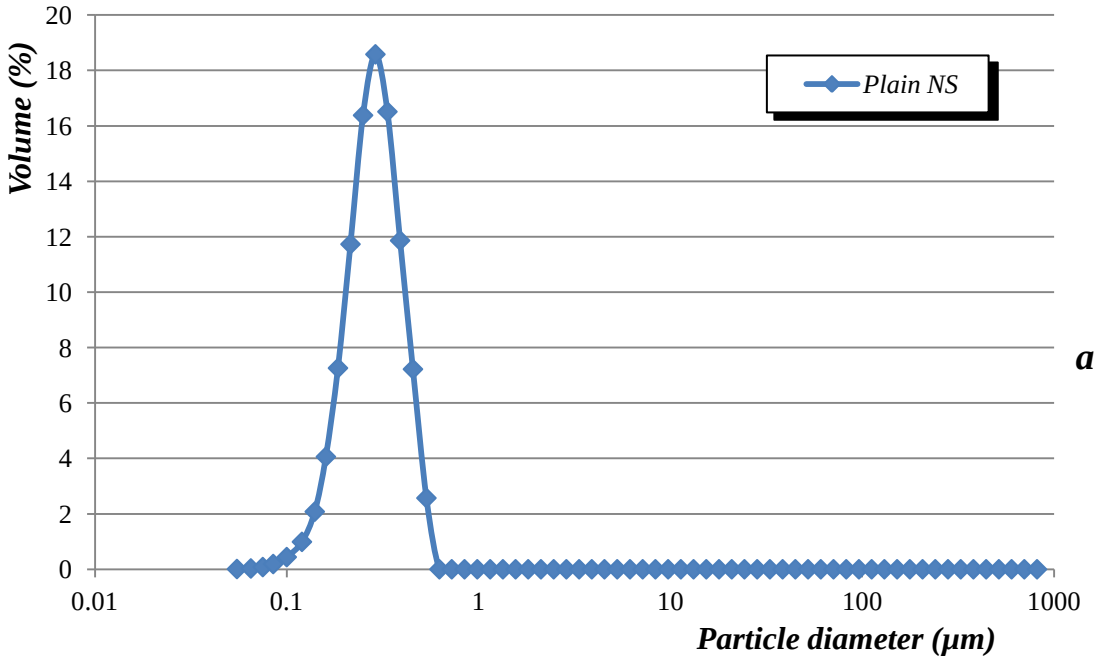
Volume (%)
20
18
16
14
12
10
8
6
4
2
0
0.01
0.1
1
10
100
1000
Particle diameter (µm)
Plain NS
a

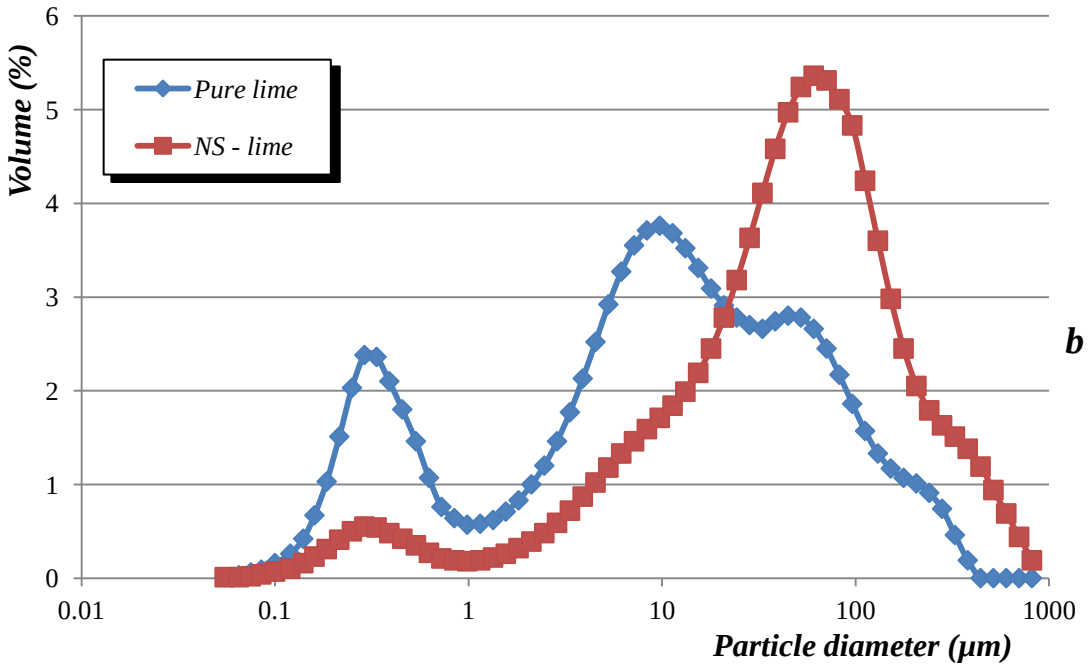
Volume (%)
6
5
4
3
2
1
0
0.01
0.1
1
10
100
1000
Particle diameter (µm)
Pure lime
NS - lime
b

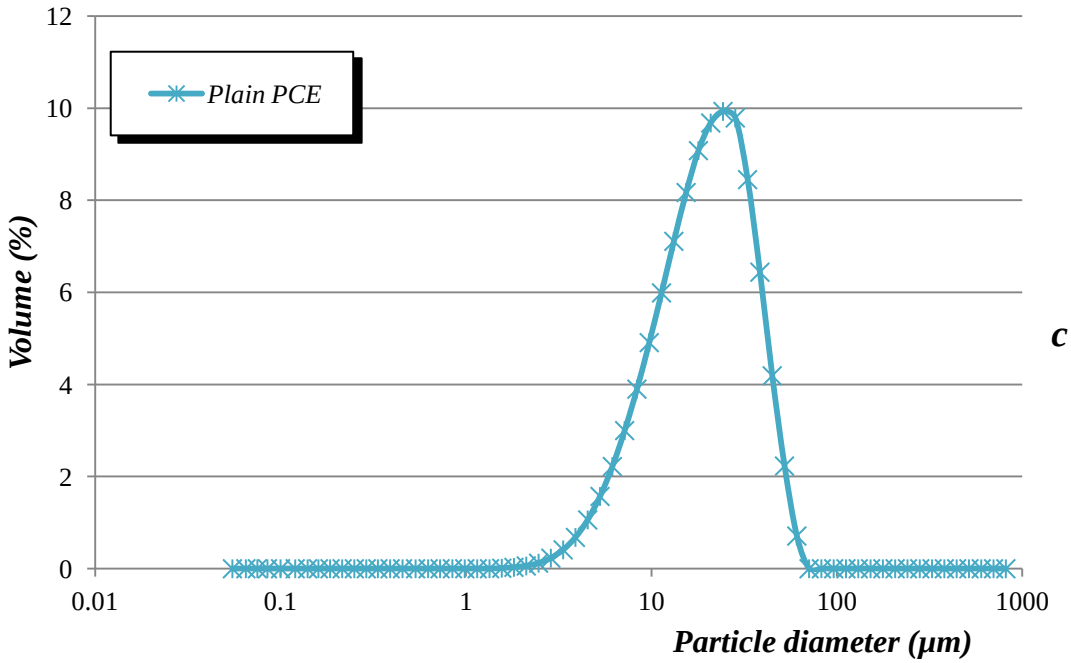
Plain PCE
Volume (%)
Particle diameter (µm)
0
2
4
6
8
10
12
0.01
0.1
1
10
100
1000

c

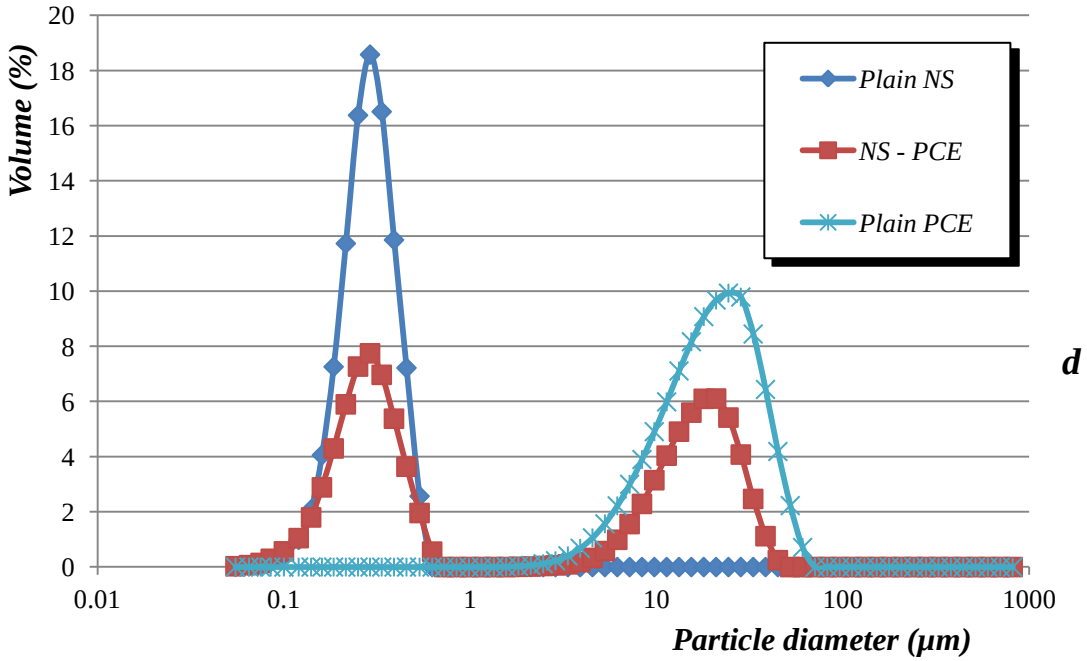
Plain NS
NS - PCE
Plain PCE
Volume (%)
Particle diameter (µm)
0
2
4
6
8
10
12
14
16
18
20
0.01
0.1
1
10
100
1000

d

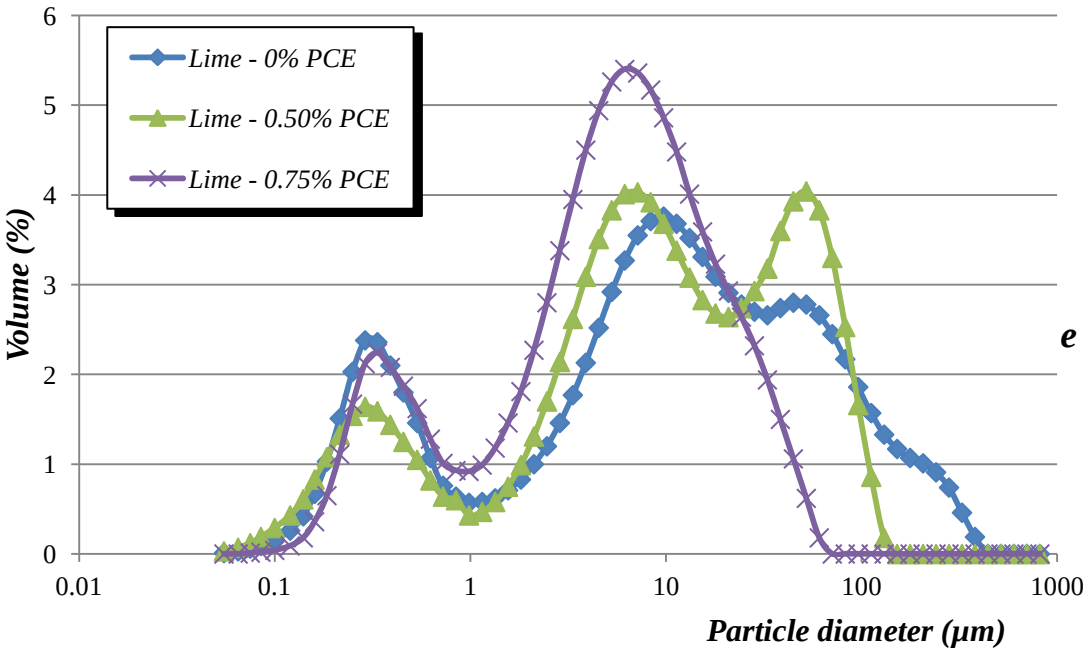

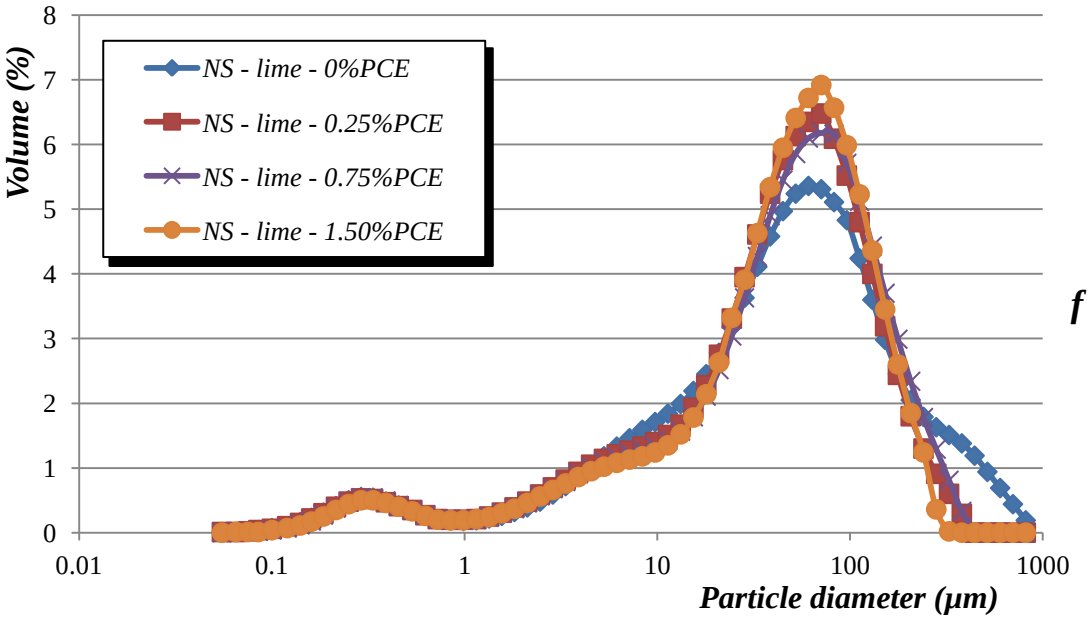

Figure 1. Particle size distributions of different suspensions: **a)** plain NS; **b)** pure lime and NS-lime (6 wt. %NS); **c)** plain PCE; **d)** combined plot of a) and c) plus a graph depicting PSD of a NS-PCE mixture, showing two peaks that perfectly match those of individual suspensions of PCE and NS, indicating the absence of interaction between NS and PCE; **e)** NS-free lime suspensions, with increasing amounts of PCE (wt. % by weight of lime); **f)** NS-lime suspensions (6 wt. %NS), in the presence of increasing amounts of PCE (wt. % by weight of lime).

Figure 2

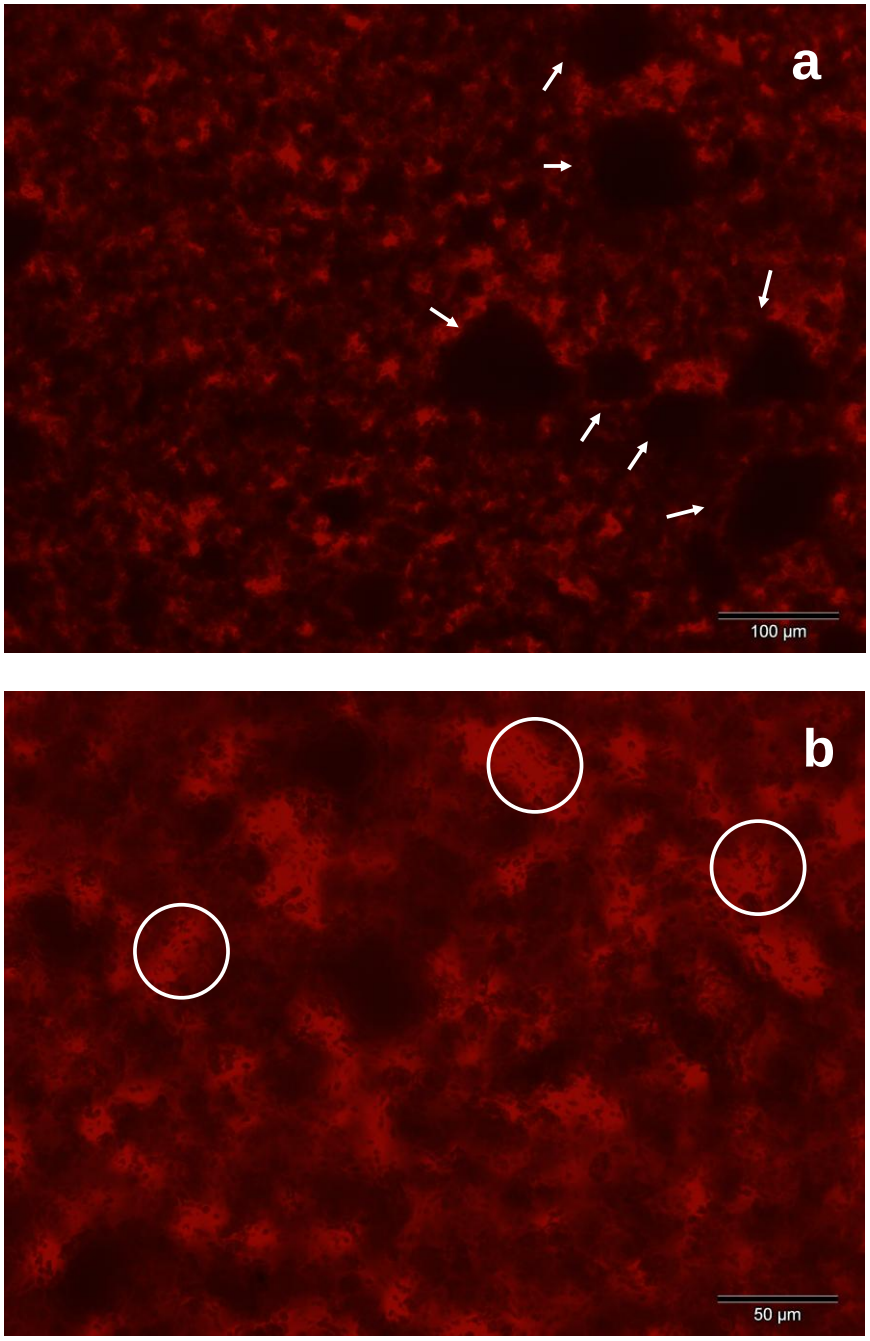

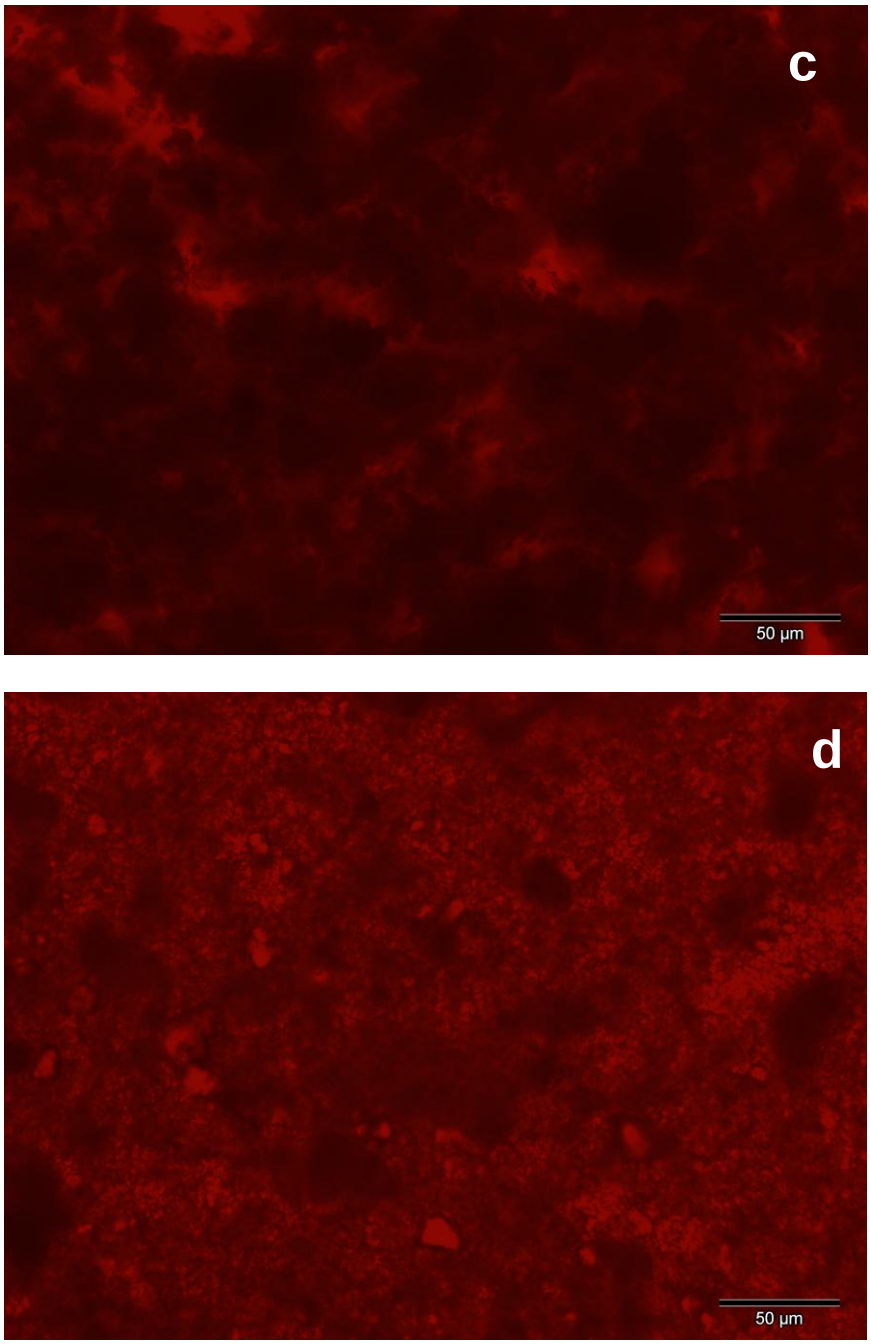

Figure 2. Optical microscopy photographs of lime suspensions: a) Pure lime suspension: white arrows show large agglomerates, depicted as darkened areas, ranging from 50 to 100 µm. A large population of 10-µm sized particles of portlandite can also be observed (black spots). b) Pure lime suspension at higher magnification. Besides of the particles of 10 µm, a significant amount of small particles of 0.3 µm was detected and areas which abound in these small particles are indicated by white circles. c) NS-lime suspension, showing a denser structure, with large agglomerates of particles. The smallest 0.3 µm-sized particles have almost disappeared. d) Lime-PCE suspension micrograph, showing small particles and the absence of large agglomerates as a result of the dispersing action of the PCE.

Figure 3

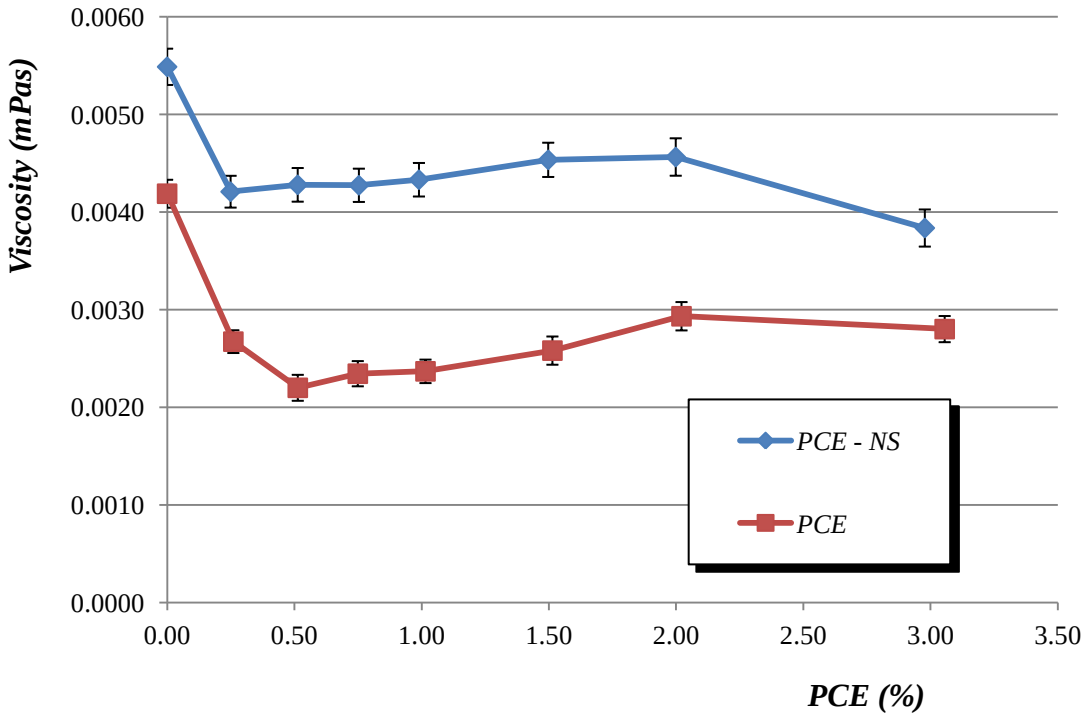

Figure 3. Viscosity measurements *vs.* PCE content for two lime suspensions: with 6 wt. % NS (blue line, diamonds) and NS-free lime suspension (red line, squares). Error bars are included for each one of the measurements.

Figure 4

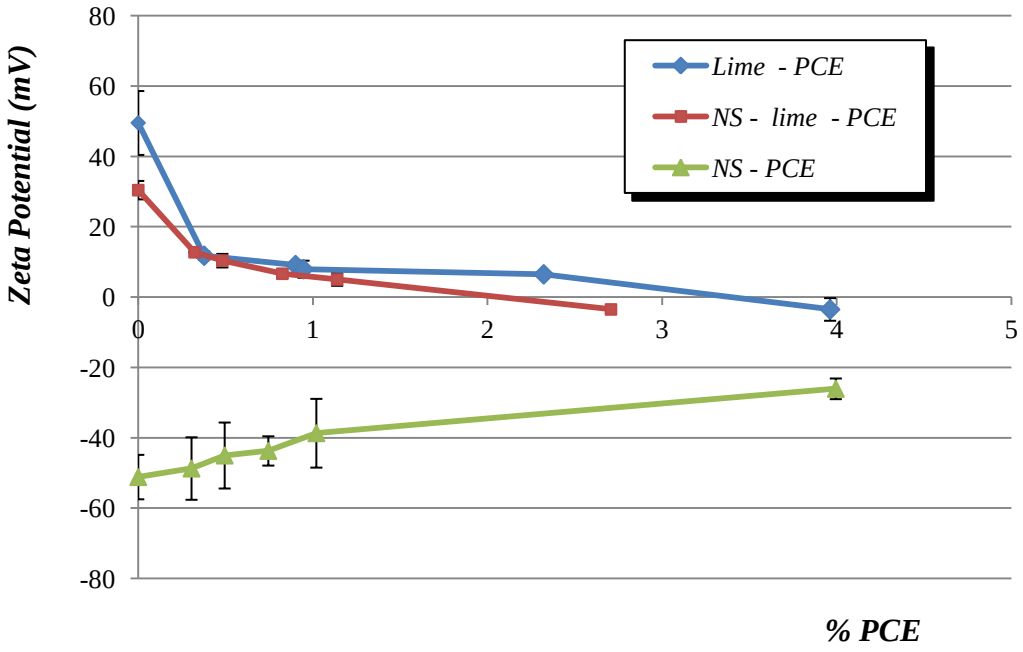

Figure 4. Zeta potential values of different solutions *vs.* increasing amounts of PCE. NS-free lime solution: blue line (diamonds). NS-lime (6 wt. % NS): red line (squares). Colloidal NS suspension: green line (triangles). Error bars are included for each one of the measurements.

Figure 5

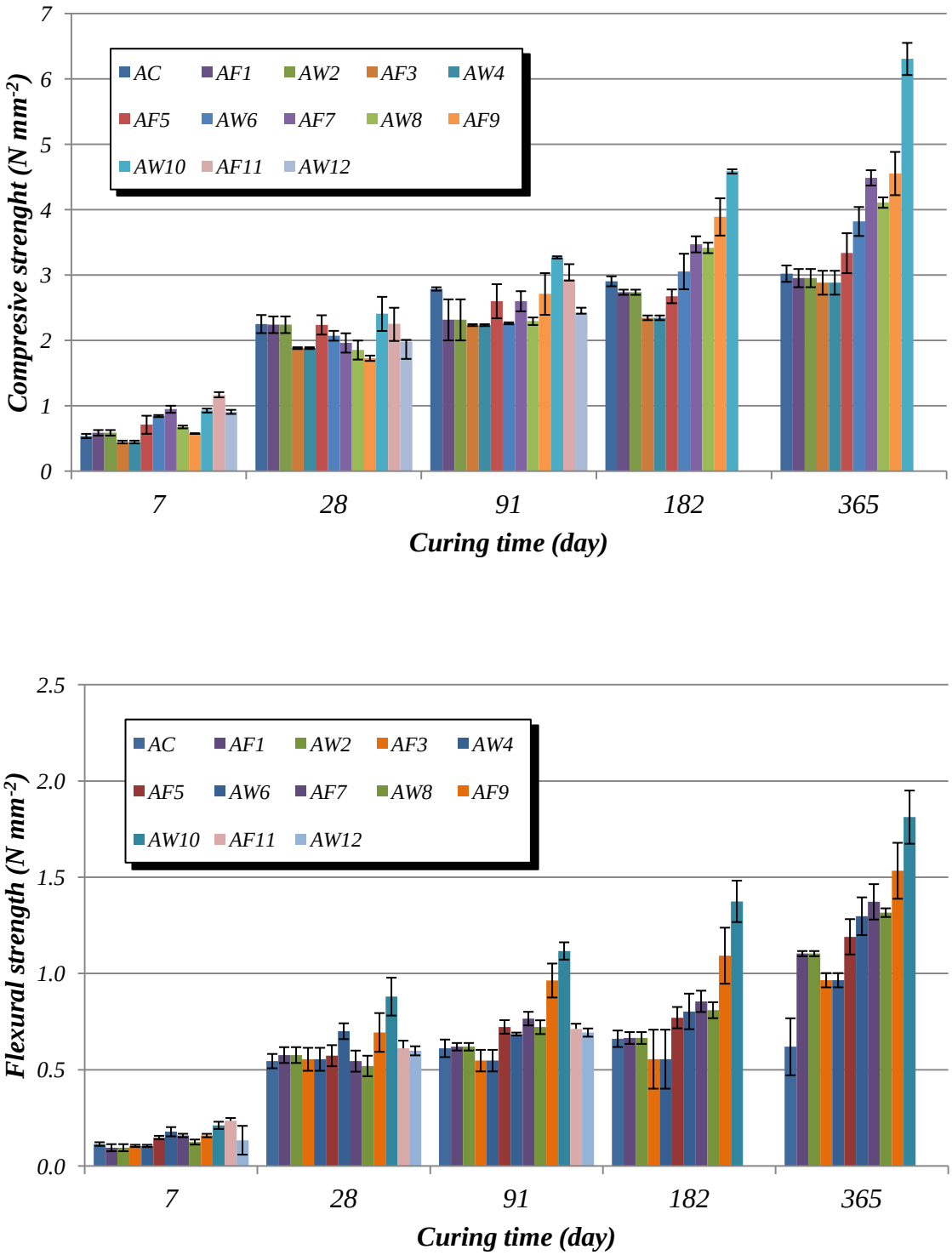

Figure 5. Compressive and flexural strength results *vs.* curing time for A samples, 1:2 binder:aggregate ratio.

Figure 6

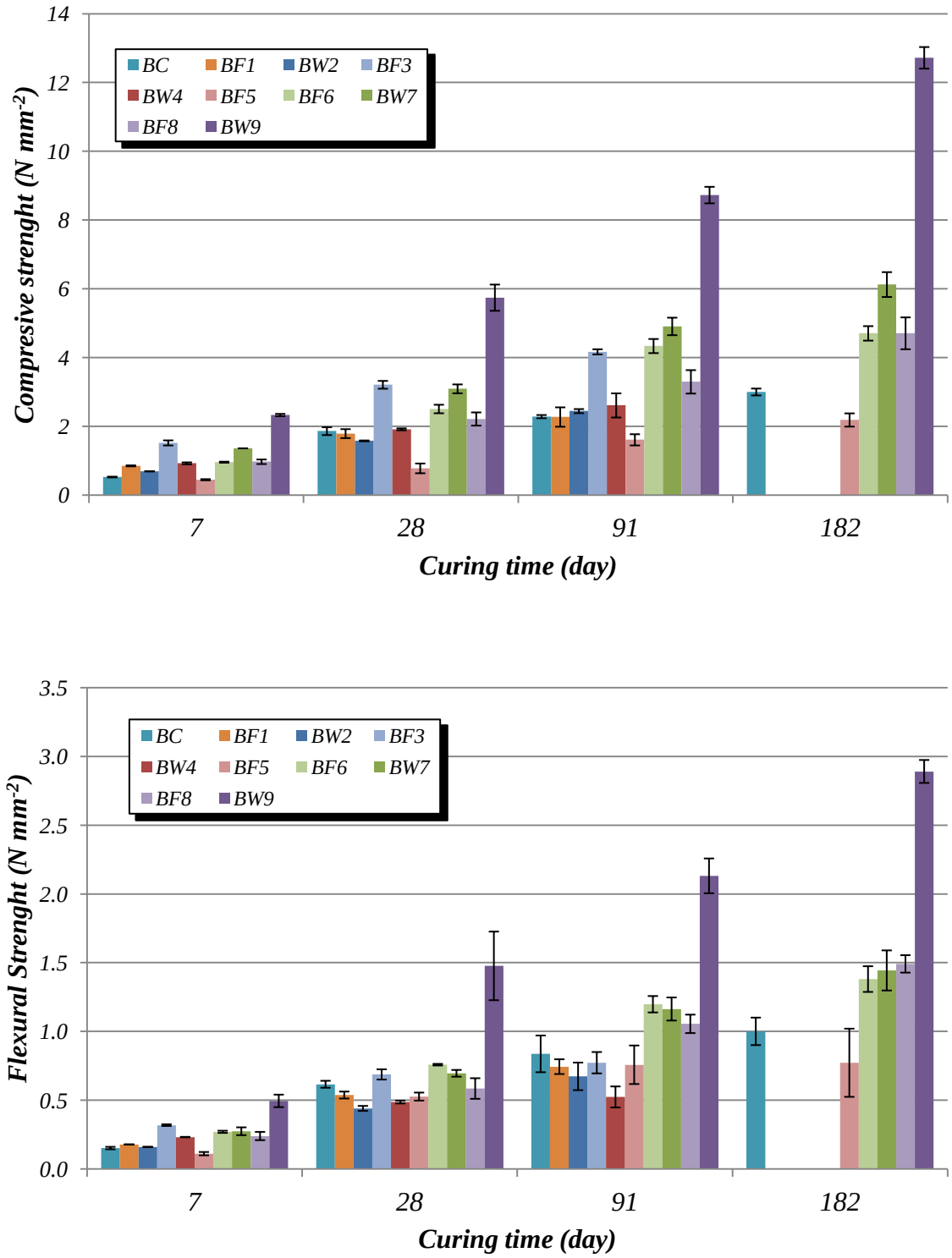

Figure 6. Compressive and flexural strength results *vs.* curing time for B samples, 1:1 binder:aggregate ratio.

Figure 7

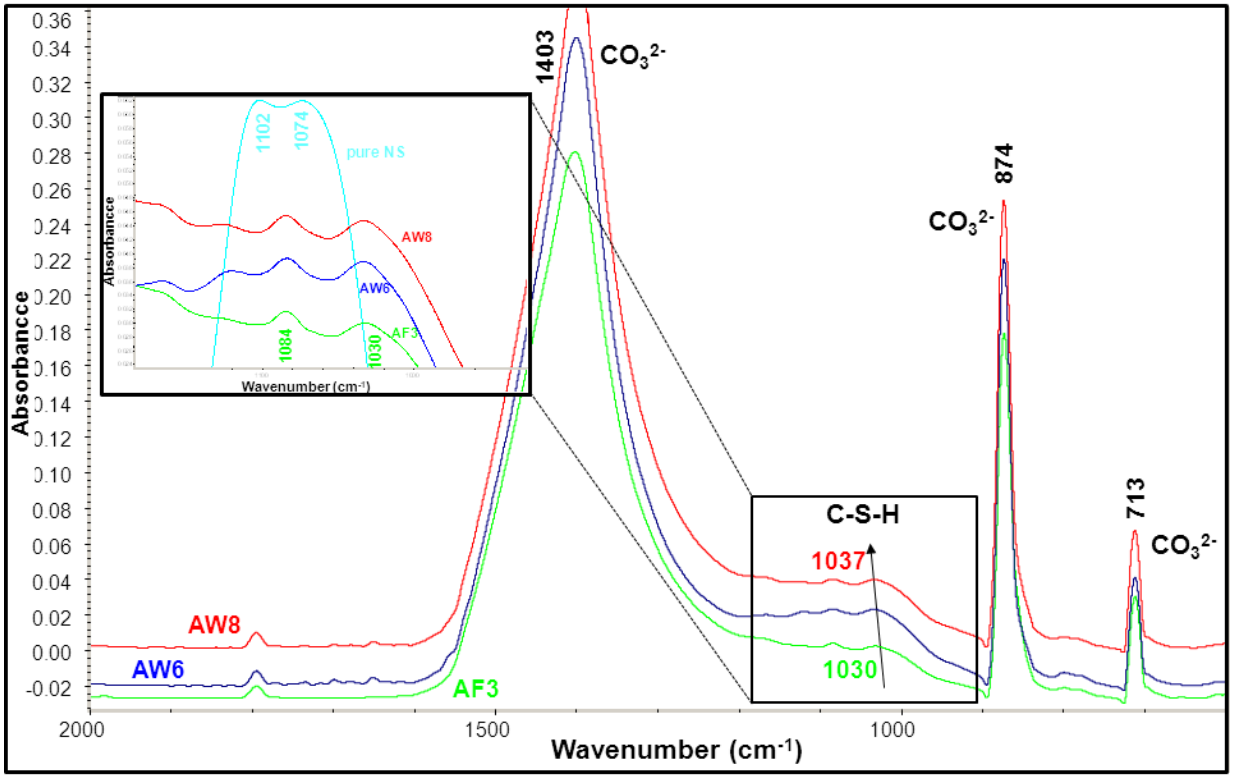

Figure 7. FTIR spectra of mortar samples modified by NS addition: AF3 (1 wt. % NS), AW6 (2 wt. % NS) and AW8 (3 wt. % NS). The shift (marked by an arrow, from 1030 to 1037 cm^{-1}) of the asymmetric stretching vibrations of the Si-O-Si group – related to CSH – indicates a higher degree of polymerization as a function of increasing amounts of NS. The other identified absorption bands correspond to carbonate groups of the calcite. An inset enlarging the region from ca. 900 to 1200 cm^{-1} is also shown, together with the spectrum of pure NS.

Figure 8

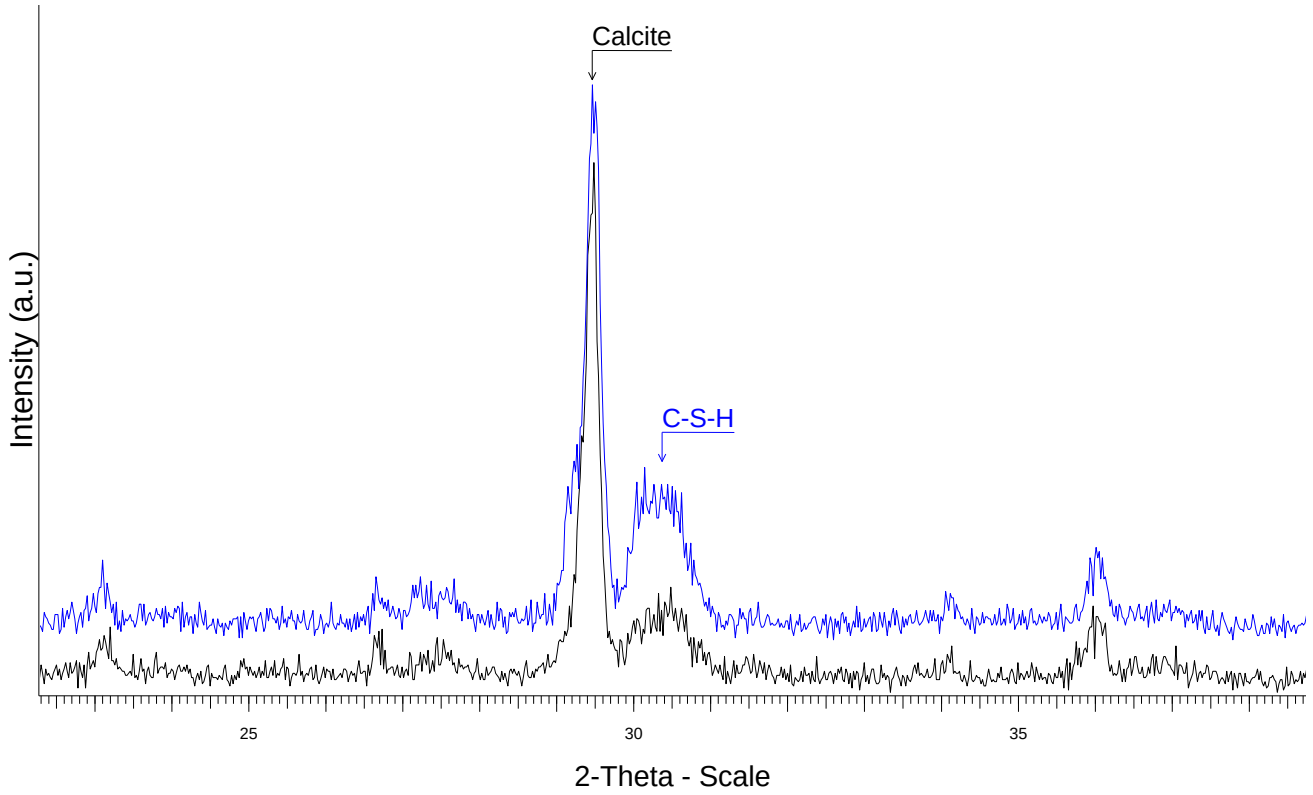

Figure 8. XRD patterns corresponding to samples AW6 (black, bottom) and AW8 (blue, top) after 182 curing days.

Figure 9

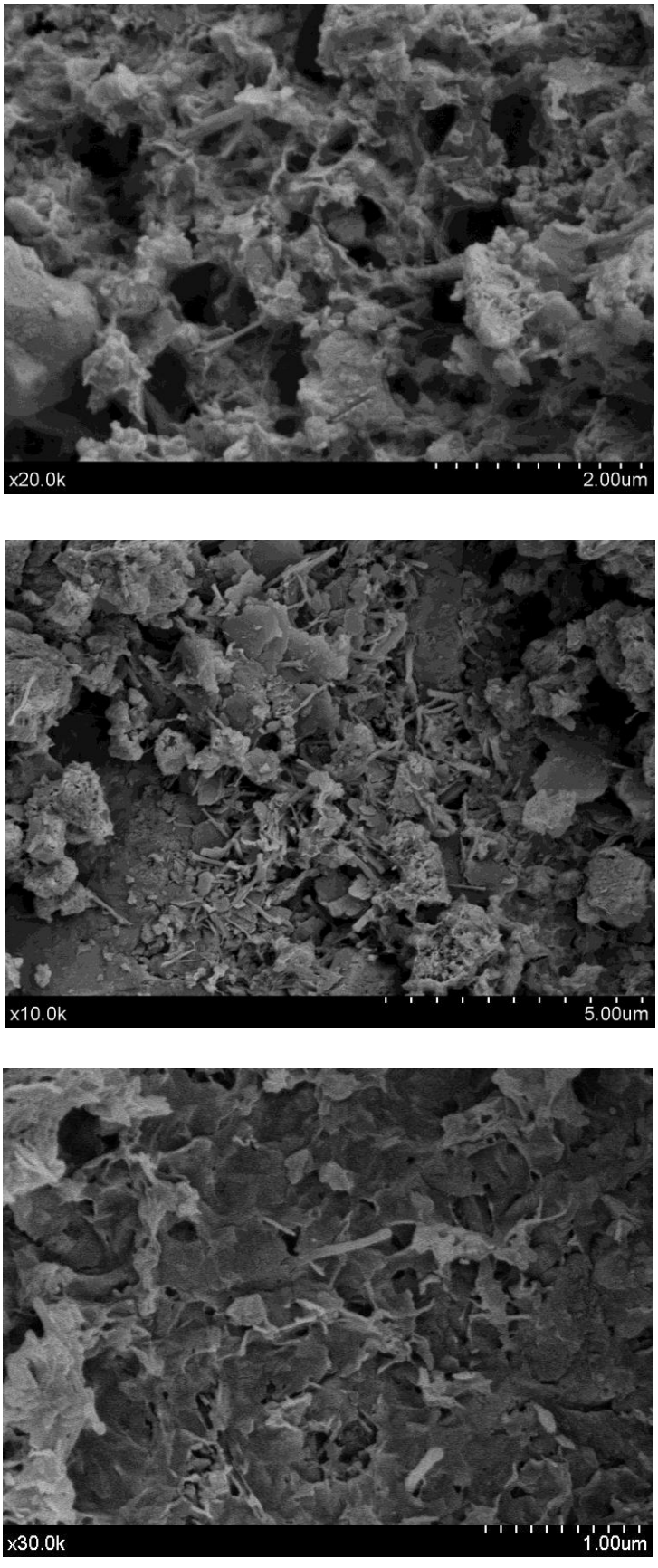

Figure 9. SEM micrographs of BF3 sample (6 wt. % NS): a) CSH area showing a honeycomb-like structure; b) CSH in a combined flakes and rods pattern; c) CSH in a thin foils-shaped form.

Figure 10

a)

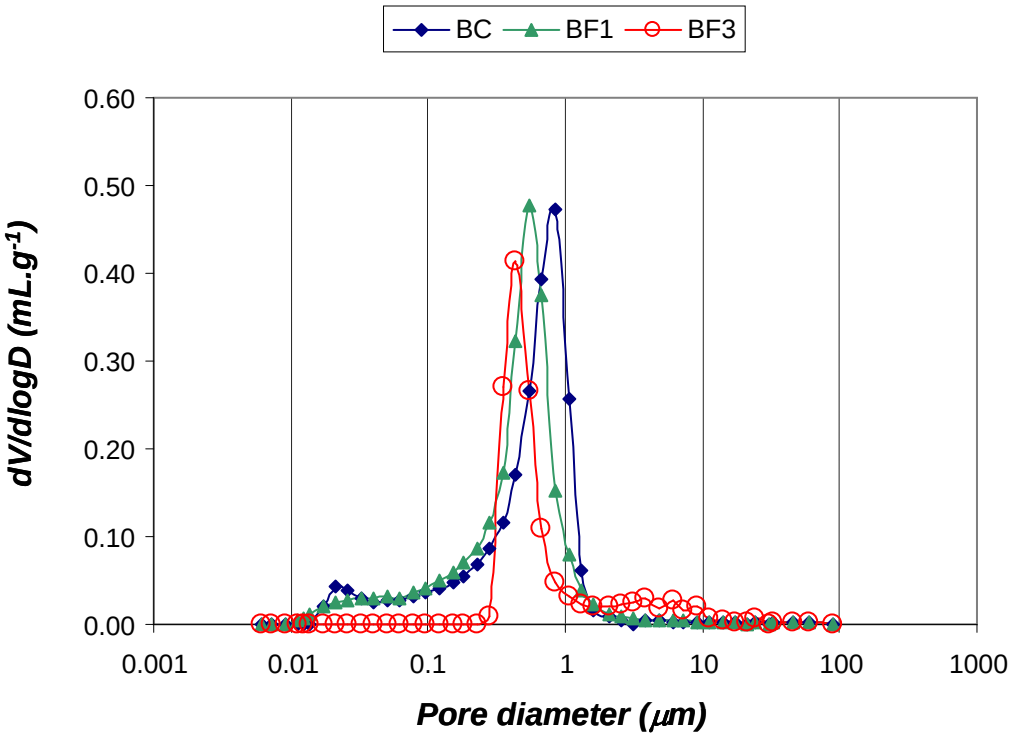
BC
BF1
BF3
0.60
0.50
0.40
0.30
0.20
0.10
0.00
dV/dlogD (mL.g-1)
0.001
0.01
0.1
1
10
100
1000
Pore diameter (μm)

b)

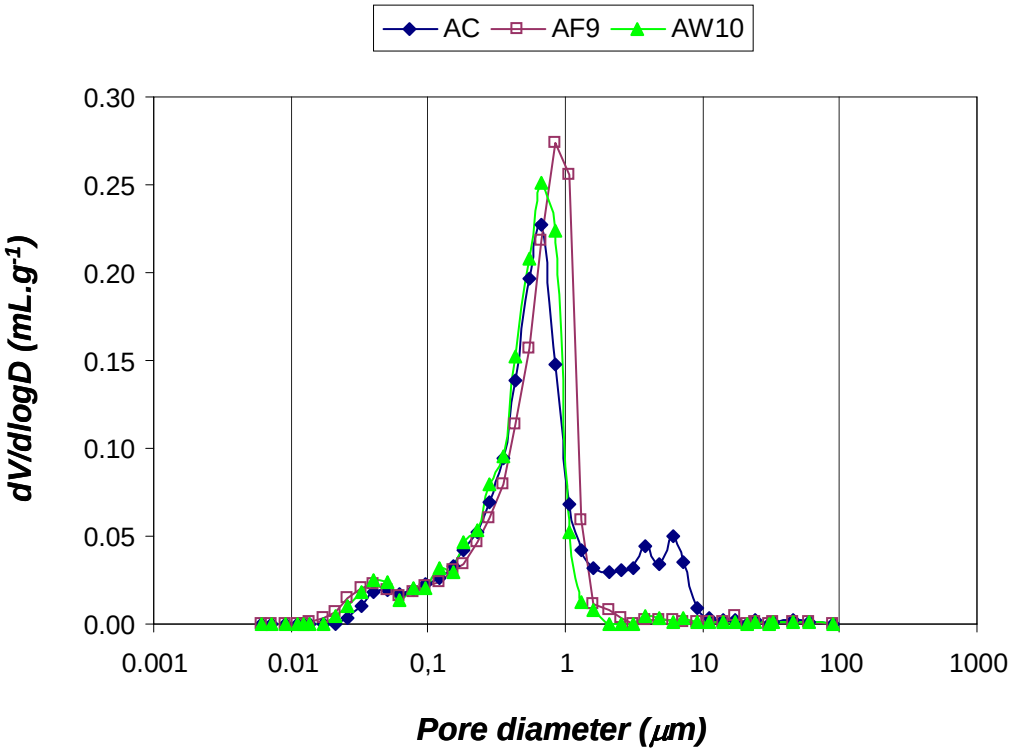
AC
AF9
AW10
0.30
0.25
0.20
0.15
0.10
0.05
0.00
dV/dlogD (mL.g-1)
0.001
0.01
0,1
1
10
100
1000
Pore diameter (μm)

c)

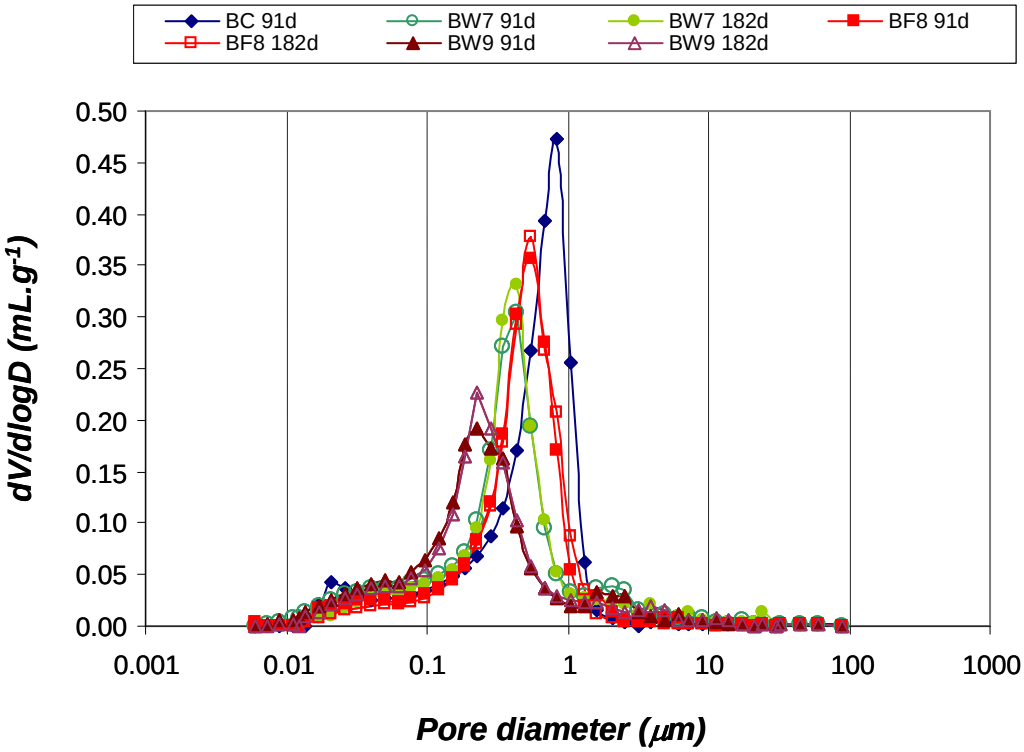

Figure 10. Pore size distribution from MIP data for: a) samples with different percentages of NS with respect to control mortar: BC (0 wt. %NS), BF1 (3 wt. %NS) and BF3 (6 wt. %NS), after 91 curing days; b) samples with PCE with respect to control mortar: AC (0 wt. %PCE), AF9 (0.5 wt. %PCE) and AW10 (0.5 wt. %PCE), after 182 curing days; c) samples with combined presence of both NS and PCE admixtures after 91 and 182 curing days, compared with control mortar: control sample BC (0 wt. % NS, 0 wt. % PCE); BW7 (6 wt. %NS, 0.5 wt. %PCE); BF8 (6 wt. %NS, 1 wt. %PCE); BW9 (6 wt. %NS, 1 wt. %PCE).

Figure 11

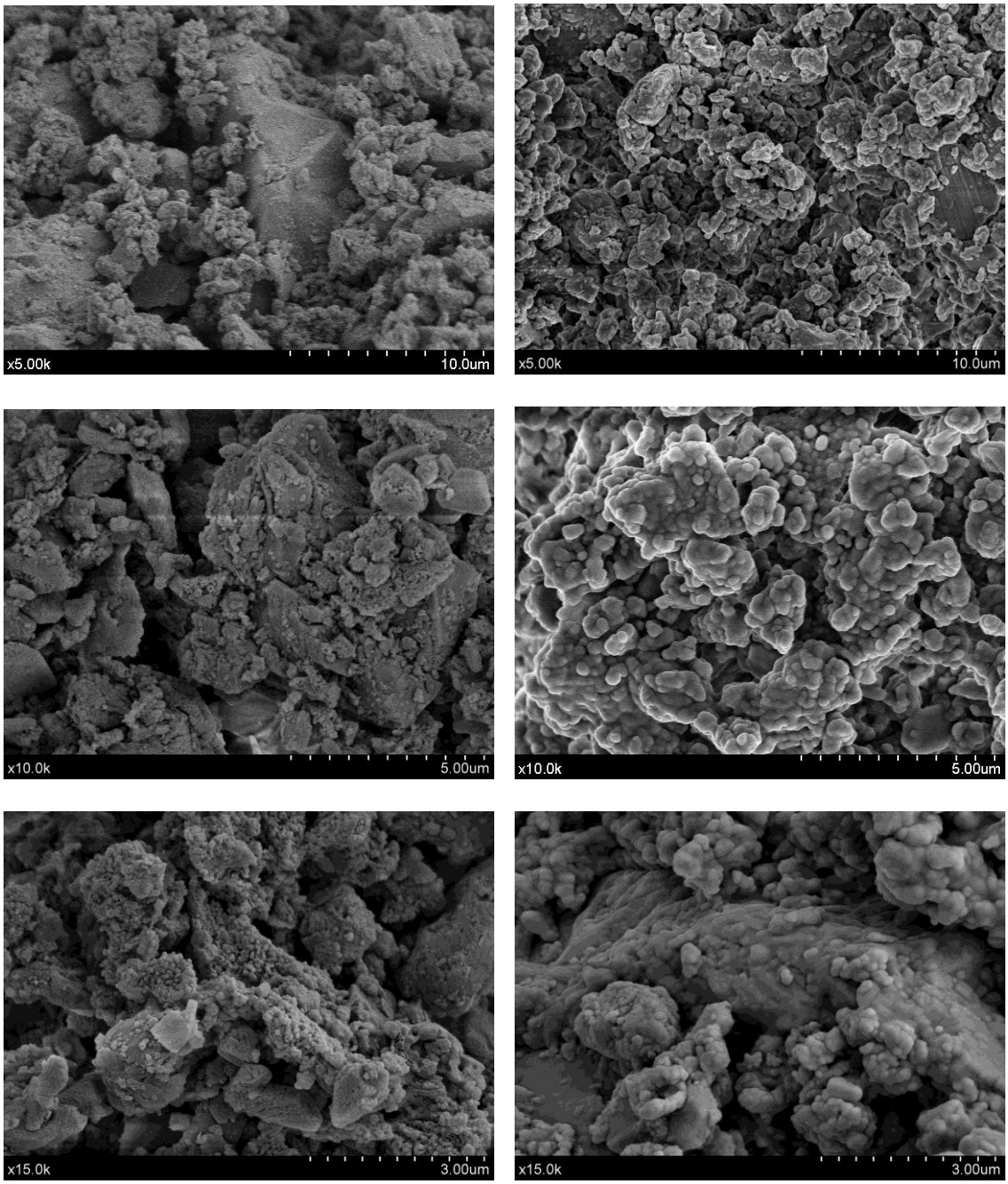

Figure 11. Comparative SEM micrographs after 91 curing days between AC control sample (on the left side) and AW10 sample with 0.5% of plasticizer (on the right side) at different magnification. Samples with PCE showed compact and large agglomerates of rounded calcite crystals and reduced porosity.

Figure 12

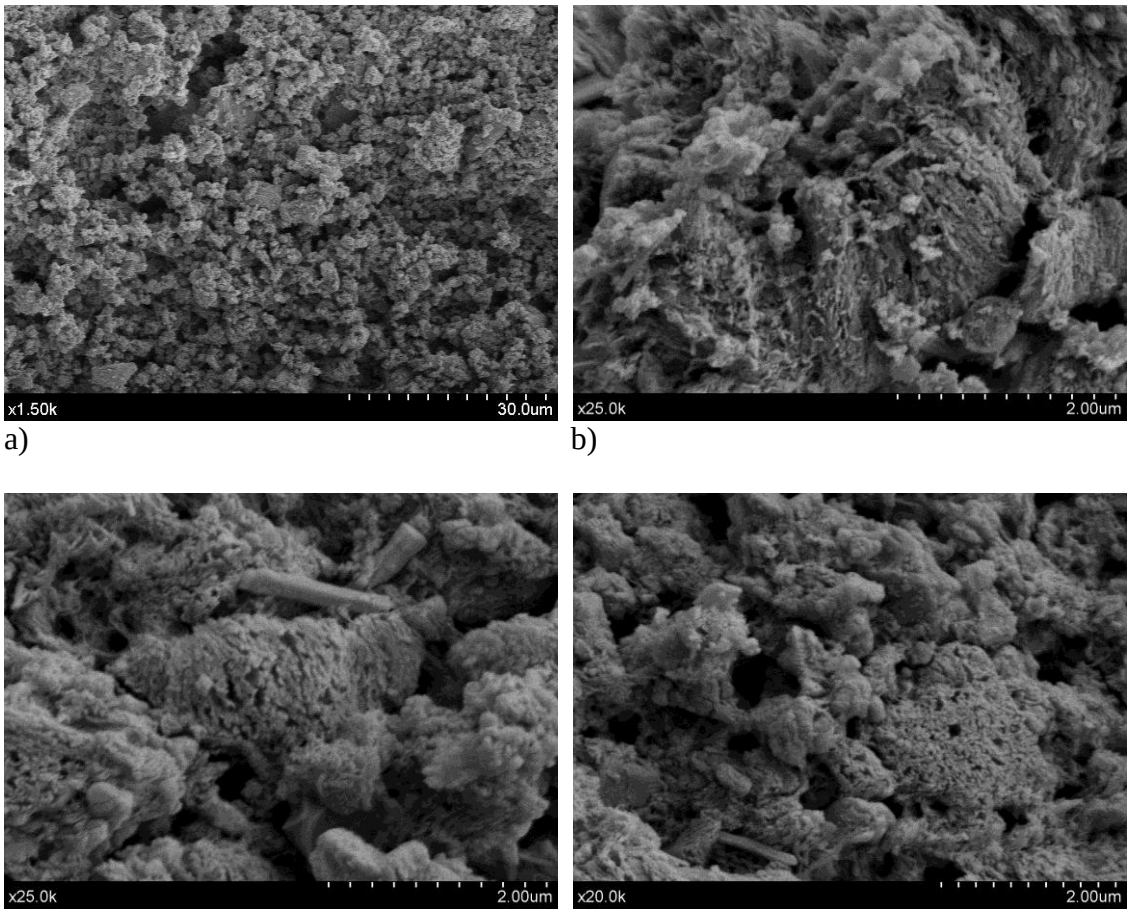

Figure 12. SEM micrographs obtained from BW9 sample after 91 curing days, showing the noticeable densification of the matrix and reduced mean pore size (a). Microstructure appears dominated by CSH structures: honeycomb forms, some rods and a network (b).In (c), other area of BW9 sample showing similar CSH structures and including some areas of rounded calcite crystals agglomeration owing to the PCE presence (on the right side of the picture). (d) Detail of BW9 sample, allowing the observation of a dense matrix and low pore size diameter.